PERGAMON

Quaternary Science Reviews 19 (2000) 1801–1820

QSR

# Holocene hydrological reconstructions from stable isotopes and paleolimnology, Cordillera Real, Bolivia

Mark B. Abbott[a,*], Brent B. Wolfe[b], Ramón Aravena[b], Alexander P. Wolfe[c], Geoffrey O. Seltzer[d]

[a]*Department of Geosciences, Morrill Science Center Box 35820, University of Massachusetts, Amherst, MA 01003-5820, USA*
[b]*Department of Earth Sciences, University of Waterloo, Waterloo, Canada ON N2L 3G1*
[c]*Institute of Arctic and Alpine Research, Campus Box 450, University of Colorado, Boulder, CO 80309-0450, USA*
[d]*Department of Earth Sciences, Heroy Geology Laboratory, Syracuse University, Syracuse, NY 13244-1070, USA*

**Abstract**

Multiproxy analyses of sediment cores from Lago Taypi Chaka Kkota (LTCK) Cordillera Real, Bolivia, provide a record of drier conditions following late Pleistocene deglaciation culminating in pronounced aridity between 6.2 and 2.3 ka B.P. Today LTCK is a glacial-fed lake that is relatively insensitive to changes in P–E because it is largely buffered from dry season draw-down through the year-round supply of glacial meltwater. This was not the case during the middle to late Holocene when glaciers were absent from the watershed. Lake-water $\delta^{18}O$ values inferred from $\delta^{18}O$ analysis of sediment cellulose range from $-12.9$ to $-5.3‰$ and average $-8.7‰$ between 6.2 and 2.3 ka B.P. Modern lake-water $\delta^{18}O$ from LTCK averages $-14.8‰$ which is compatible with the $\delta^{18}O_{lw}$ value of $-14.3‰$ for the surface sediment cellulose. Analyses of $\delta^{18}O$ from modern surface waters in 23 lakes that span the range from glacial-fed to closed basin vary from $-16.6$ to $-2.5‰$. This approximates the magnitude of the down-core shift in $\delta^{18}O_{lw}$ values in LTCK during the middle to late Holocene from $-12.9$ to $-5.3‰$. Strong paleohydrologic change during the middle Holocene is also evident in diatom assemblages that consist of shallow-water, non-glacial periphytic taxa and bulk organic $\delta^{13}C$ and $\delta^{15}N$ that show increases likely resulting from degradation of lacustrine organic matter periodically exposed to subaerial conditions. Neoglaciation began after 2.3 ka B.P. as indicated by changes in the composition of the sediments, lower $\delta^{18}O$ values, and a return to diatom assemblages characteristic of the glacial sediments that formed during the Late Pleistocene. Collectively, these data indicate that the past 2.3 ka B.P. have been the wettest interval during the Holocene. Millennial-scale shifts in the paleohydrologic record of LTCK during the early to middle Holocene conform to other regional paleoclimatic time-series, including Lake Titicaca and Nevado Sajama, and may be driven by insolation and resultant changes in atmospheric circulation and moisture supply. In contrast, an apparent 1200-year lag in the onset of wetter conditions at LTCK (2.3 ka B.P.) compared to Lake Titicaca (3.5 ka B.P.) provides evidence for variable sub-regional hydrologic response to climate change during the middle to late Holocene. © 2000 Elsevier Science Ltd. All rights reserved.

## 1. Introduction

As we become increasingly aware of the international significance and economic importance of present and future climate changes, we must focus on the potential mechanisms for both natural and anthropogenic environmental change. The emphasis of most current research is to reconstruct past temperature changes, but fluctuations in the precipitation–evaporation (P–E) balance have equally important implications to society and have recently been shown to occur over time-scales relevant to humans (e.g. Hodell et al., 1995; Abbott et al., 1997b; Binford et al., 1997). Most important, perhaps, is that emphasis be placed on determining when, where, and how fast climate has varied during the Holocene when overall boundary conditions were similar to today. By documenting the spatial and temporal pattern of Holocene climatic change from a network of sites in the Andes we will be better able to forecast future changes in regional hydrology.

The Andean altiplano and surrounding cordillera have experienced major hydrological changes during the late Pleistocene and Holocene as documented by a variety of paleoclimate records including glacial geology, pluvial lakes, and cores from Lake Titicaca. Seltzer (1990, 1992)

* Corresponding author. Tel.: +1-413-545-0229; fax: +1-413-545-1200.
*E-mail address:* mabbott@geo.umass.edu (M.B. Abbott).

0277-3791/00/$ - see front matter © 2000 Elsevier Science Ltd. All rights reserved.
PII: S0277-3791(00)00078-0

showed that deglaciation occurred rapidly during the latest Pleistocene with no evidence for Holocene glaciation until relatively minor Neoglacial readvances of less than 200 m extent. Pluvial lake studies indicate that high lake stands on the altiplano lasted until about 9.5 ka B.P. with no evidence of subsequent high water levels (Grosjean et al., 1995; Clayton and Clapperton, 1997). Studies of sediment cores from Lake Titicaca indicate that the water level was at least 50 m lower 8.4 ka B.P. (Wirrmann and De Oliveira Almeida, 1987) and probably as much as 100 m lower than today at this time (Seltzer et al., 1998; Cross et al., 2000). After 3.5 ka B.P. water level rose to the overflow level with four low water stands from 3.5 ka B.P. to present (Wirrmann and Mourguiart, 1995; Abbott et al., 1997b; Mourguiart et al., 1998). Together, these studies indicate that the region became increasingly arid from the late Pleistocene to the middle Holocene with wetter conditions starting around 4 ka B.P.

None of these climate archives, however, are continuous. Ice cores collected on Nevado Sajama in the western cordillera provide continuous records and suggest that warm-dry conditions began at 15.5 ka B.P., but were interrupted by cold–wet conditions between 14.3 and 11.5 ka B.P. (Thompson et al., 1998). This finding is not consistent with the regional record of deglaciation and pluvial lake levels which both suggest rapid deglaciation between 14 and 10 ka B.P. During the Holocene the Sajama record suggests arid conditions from $\sim$ 9 to 3 ka B.P. and wetter conditions thereafter. The high resolution record from the Sajama ice core contains a tremendous amount of paleoclimate information, but interpretation of ice core $\delta^{18}O$ results are complicated because the signal incorporates changes in temperature, precipitation source, and evaporative enrichment by sublimation (Grootes et al., 1989).

Here we present a multi-proxy study on a sediment core from Lago Taypi Chaka Kkota (LTCK) detailing major shifts in watershed hydrology during the Holocene that are primarily driven by changes in the P–E balance. This study is an extension of preliminary work by Abbott et al. (1997a) that detailed the sedimentology of the same site. New results described here include stable isotope measurements on sediment cellulose ($\delta^{18}O$ and $\delta^{13}C$) and bulk sediment ($\delta^{13}C$ and $\delta^{15}N$), and analysis of diatom assemblages. These results are compared with other paleoclimate records in the region to assess the consistency of the emerging paleoclimate history of the region.

Oxygen and carbon isotope analyses on the fine-grained ( $< 500$ μm) cellulose fraction of lacustrine organic matter are an effective tool for reconstructing hydrological conditions and carbon pathways in lake watersheds (e.g., MacDonald et al., 1993; Duthie et al., 1996; Wolfe et al., 1996). Aquatic plant cellulose is a particularly useful substrate because its oxygen isotope composition is consistently enriched by 27 to 28‰ compared to water and is unaffected by changes in temperature (DeNiro and Epstein, 1981; Sternberg, 1989; Yakir, 1992). Therefore, with no temperature-dependant fractionation, interpreting cellulose $\delta^{18}O$ paleorecords is more straightforward than carbonate records. Interpretation is simplified because only two factors control the $\delta^{18}O$ signal: (1) the isotopic composition of input waters that are determined by precipitation, surface runoff, and groundwater and (2) hydrologic processes that modify the isotopic composition of meteoric water, such as evaporation. If you can assume a purely lacustrine origin of cellulose, lake-water $\delta^{18}O$ histories can be directly inferred from cellulose $\delta^{18}O$ and provide information on watershed hydrology. In this study we incorporate regional sampling and isotopic analysis of modern lake water in different hydrologic settings as a means to interpret down-core profiles of the cellulose-inferred lake water $\delta^{18}O$. In addition, changes in diatom floras were used to document down-core changes in periphytic and glacial lake assemblages.

## 2. Field area and climate

### 2.1. Regional climatic setting

Precipitation in the altiplano region and the surrounding cordillera is marked by pronounced seasonal contrasts. During the Austral summer months (December–March) a heat-induced low-pressure cell forms over the center of the South American continent that draws moisture from the South Atlantic. At the same time, convective activity over the altiplano associated with the "Bolivian High" (Aceituno and Montecinos, 1993) produces summer precipitation in the Andes accounting for 65 to 78% of the annual total. At the higher elevations this precipitation occurs as snow. Periodic blocking of the easterly atmospheric circulation by the westerlies (Aceituno and Montecinos, 1993; Kessler, 1988) and perturbations caused by El Niño Southern Oscillation (ENSO) events (Thompson et al., 1984; Ribstein et al., 1995; Francou et al., 1995) are conditions that result in unusually dry conditions on the altiplano during the summer. We contend that the synoptic climatic conditions that lead to seasonal and intra-seasonal variations in effective moisture today on the altiplano serve as appropriate analogues for changes that may have occurred over longer periods during the Holocene.

The eastern cordillera of the northern Bolivian Andes is characterized as a zone of steep climatic gradients caused by the marked gain in altitude from the Amazon Basin to mountain peaks exceeding 6000 m elevation. The result is a pronounced rain shadow, with precipitation decreasing east to west from $> 1400$ mm yr$^{-1}$ in the lowlands to less than 700 mm yr$^{-1}$ on the altiplano

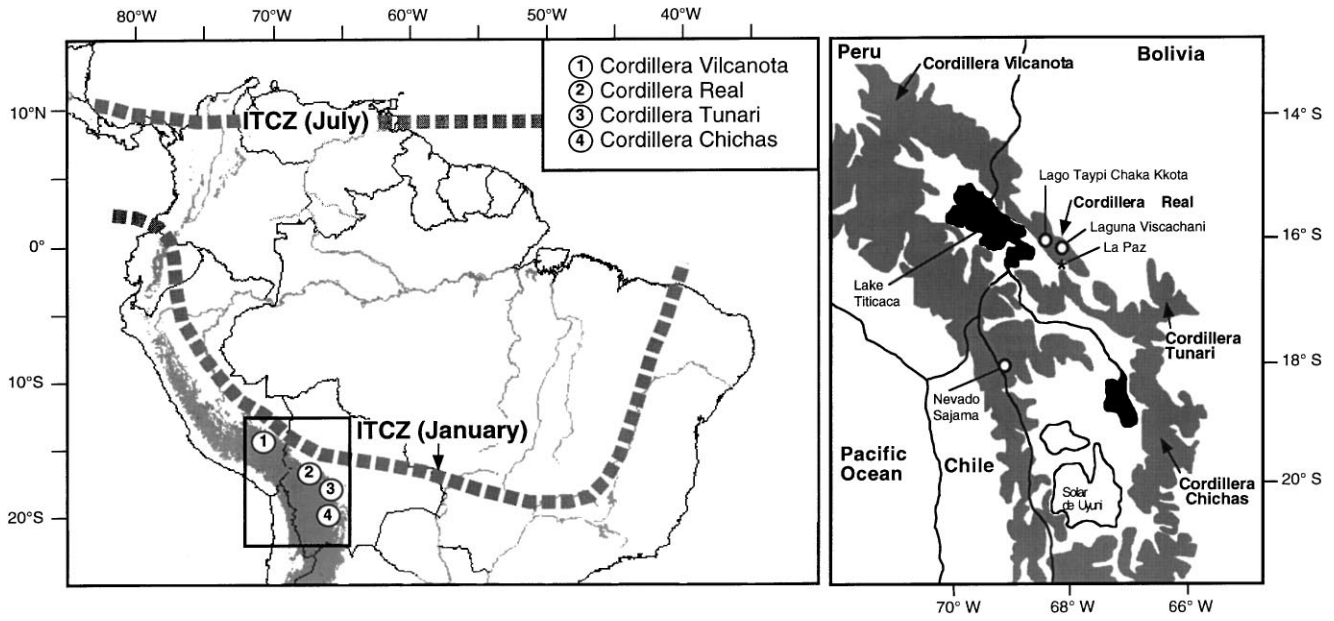


Fig. 1. Location of the study site in Bolivia. Average summer locations of the Intertropical Convergence Zone (ITCZ) during January and July are shown by the thick dashed lines. The study area in the Bolivian Andes has a summer wet season and is located at the southernmost extension of the ITCZ. Shaded area represents elevations greater than 3000 m. Modern lake-water samples were collected from the Cordillera Vilcanota, Real, Tunari, and Chichas.

(Hoffman, 1975). Roche et al. (1992) estimated that the highest peaks of the eastern Cordillera Real receive more than 800 mm $yr^{-1}$ of precipitation, whereas 50 km to the west this decreases to less than 500 mm/$yr^{-1}$. Ribstein et al. (1995) measured $\sim$900 mm of precipitation during the 1992–1993 hydrological year on the Zongo Glacier in the Cordillera Real, situated 20 km to the south of LTCK.

### 2.2. Late Quaternary evolution of the Rio Palcoco valley

The LTCK watershed is located at 16°13′S, 68°21′W in the Rio Palcoco Valley on the western slope of the Cordillera Real (Fig. 1). LTCK is situated at 4300 m elevation and is lowest in a chain of three lakes. The cirque headwalls up-valley attain 5650 m elevation and contain a series of small alpine glaciers. Seltzer (1992) described rapid deglaciation of the Rio Palcoco valley on the basis of a series of concordant bulk sediment $^{14}C$ dates obtained from the base of the organic-rich sediments distributed between the headwall and 10 km down valley. Glaciers receded to within their Neoglacial limits by 9.5 ka B.P. as indicated by a radiocarbon date on peat overlying glacial silt from a bog proximal to the modern glacier terminus at 4670 m elevation (Seltzer, 1992). Late Holocene glacial advances in the Cordillera Real were modest, extending less than 200 m from modern termini (Gouze et al., 1986; Seltzer, 1990). This is compatible with sedimentological evidence from LTCK that suggests that glaciers were not present in the watershed during the middle Holocene (Abbott et al., 1997a).

## 3. Methods

### 3.1. Coring and sediment processing

Cores were taken from the central basin of the lake with a square-rod piston corer (Wright et al., 1984) and a piston corer designed to collect undisturbed the sediment–water interface (Fisher et al., 1992). Laboratory analyses were focused on the upper 3 m of the 5.3 m long Core E which was recovered from the center of the lake in 8.3 m of water. The lower 2.3 m of core contains inorganic silts similar to the basal samples of the 3 m section described in this paper. The sediment units are labeled 1–5 and described below in order of formation. A detailed description of the core sedimentology, physical characteristics, magnetic properties, and accumulation rates of organic matter, biogenic silica, and mineral matter can be found in Abbott et al. (1997a). Whole core magnetic susceptibility was measured at 1 cm increments after which cores were split, described, and photographed. Magnetic susceptibility was measured with a Bartington Susceptibility Bridge, corrected for mass differences with bulk density measurements. Half of the core was archived in ODP D-tubes at the University of Massachusetts and the other half sampled for bulk density, mass magnetic susceptibility, carbon concentration by coulometry, bulk sediment stable isotopes ($\delta^{13}C$ and $\delta^{15}N$), sediment cellulose stable isotopes ($\delta^{18}O$ and $\delta^{13}C$), diatoms, and biogenic silica. Core lithology was determined from smear-slide mineralogy and detailed inspection of sediments. Munsell color, texture,

sedimentary structures, and biogenic features were also noted.

### 3.2. Geochemical and isotopic analyses

Biogenic silica analyses were performed by time-series dissolution experiments (DeMaster, 1981). Total carbon (TC) and total inorganic carbon (TIC) were measured with a UIC Coulometric System at the Limnological Research Center, University of Minnesota. Total organic carbon (OC) was calculated by the difference of TC-TIC. Lake sediment subsamples for organic elemental and isotope analysis were treated with 10% HCl to remove carbonate material, rinsed repeatedly with distilled water, lyophilized, and passed through a 500 μm sieve to remove coarse debris. Carbon and nitrogen concentration and isotopic composition of this residue were determined on a continuous flow-isotope ratio mass spectrometer (CF-IRMS) equipped with an elemental analyzer. Additional sample pretreatment including solvent extraction, bleaching, and alkaline hydrolysis removed non-cellulose organic constituents (Edwards et al., 1997). Cellulose carbon isotope composition was measured by CF-IRMS, and $CO_2$ gas collected by pyrolysis of cellulose was measured for oxygen isotope composition using a VG Prism II mass spectrometer (Edwards et al., 1994). Oxygen and hydrogen isotope analyses were conducted on a series of water samples from 23 alpine lakes surveyed in 1997 on a transect from 14 to 19°S (see Fig. 1 for locations). Water samples were analyzed using standard methods (Epstein and Mayeda, 1953; Coleman et al., 1982). Pretreatment and analysis of lake sediment and water samples were performed at the University of Waterloo. Preparation and isotopic analyses of modern vegetation and surface sediment samples followed similar procedures as the lake sediment pretreatment. All lake sediment samples were analyzed at the University of Waterloo while vegetation samples were measured at both the University of Waterloo and the University of Alaska as noted in Table 3.

Results of stable isotopic analyses are reported in δ-notation ($\delta = [(R_{sample}/R_{standard}) - -1] \times 1000$, where $R = {}^{18}O/{}^{16}O$, ${}^{15}N/{}^{14}N$, ${}^{13}C/{}^{12}C$, and ${}^{2}H/{}^{1}H$, with respect to the international standards for $\delta^{18}O$ (Vienna Standard Mean Ocean Water (VSMOW)), $\delta^{13}C$ (Vienna Peedee Belemnite (VPDB)), $\delta^{15}N$ (atmospheric nitrogen (AIR)), and $\delta^{2}H$ (Vienna Standard Mean Ocean Water (VSMOW)). Duplicate bulk organic and cellulose $\delta^{13}C$ and bulk organic $\delta^{15}N$ analyses are within $\pm 0.5‰$, while repeated cellulose $\delta^{18}O$ analyses are within $\pm 1.0‰$, reflecting both method uncertainty and sample heterogeneity. Analytical uncertainties are $\pm 0.2$ and $\pm 2.0‰$ for $\delta^{18}O$ and $\delta^{2}H$ values of water, respectively. Stable isotope measurements on sediment cellulose discussed in this paper are reported as $\delta^{18}O_{cell}$ or $\delta^{13}C_{cell}$. Likewise, stable isotope measurements on bulk sediment are reported as $\delta^{13}C_{org}$ and $\delta^{15}N_{org}$. Lake water $\delta^{18}O$ ($\delta^{18}O_{lw}$) is inferred from $\delta^{18}O_{cell}$ values using a cellulose–water oxygen isotope fractionation factor of $1.028 \pm 0.001$ (Epstein et al., 1977; DeNiro and Epstein, 1981).

### 3.3. Diatoms

Volumetric subsamples (1.0 $cm^3$) were prepared for diatom analysis by digestion in hot 30% $H_2O_2$. Diluted aliquots of cleaned slurries were evaporated at room temperature onto coverslips and mounted to slides with Naphrax medium. Valve sums of 300–500 were tallied under oil immersion (1000X) with an Olympus research microscope equipped with differential interference contrast optics. Raw count data were compiled into relative frequencies to illustrate stratigraphic changes in diatom communities. Diatom valve concentrations were evaluated by the addition of a calibrated *Eucalyptus* spike (Wolfe, 1997). Diatom taxonomy followed primarily the floras of Hustedt (1959), Germain (1981), Patrick and Reimer (1966, 1975), and Krammer and Lange-Bertalot (1986)–1991). There are many remaining enigmatic taxa, especially in the genera *Gomphonema*, *Fragilaria* and *Nupela*. A full taxonomic account is given in Appendix A.

The relative frequencies of dominant diatoms were analyzed numerically by indirect ordination using detrended correspondence analysis (DCA; Hill and Gauch, 1980), which illustrates the underlying structure of the data set by defining synthetic variables (axes) to which taxonomic abundances exhibit unimodal responses (ter Braak, 1987). The primary axes produced by DCA can frequently be interpreted ecologically; additionally, recurrent taxonomic associations can be investigated. Only taxa exceeding 1% relative frequency in at least one sample were used in the DCA (42 taxa). A square-root transformation was first applied to the diatom frequencies to moderate the influence of the most prevalent taxa. The analysis was run under the MVSP (v. 2.1) program (Kovach, 1993).

### 3.4. Geochronology

Terrestrial macrofossils were not present in sufficient quantities for $^{14}C$ dating. There are no carbonates in the LTCK watershed suggesting hardwater effects are minimal. The contemporary radiocarbon reservoir was assessed by measuring the $^{14}C$ activity of samples of living submerged *Isoetes*. These results average 114% f.M. (fraction Modern) which, for the year A.D. 1992, is indistinguishable from atmospheric $^{14}C$ activity. This suggests that lake reservoir effects are minimal and that aquatic plants are reliable targets for $^{14}C$ dating in this system. Therefore, we used *Isoetes* macrofossils for AMS $^{14}C$ measurements. Radiocarbon ages are reported with

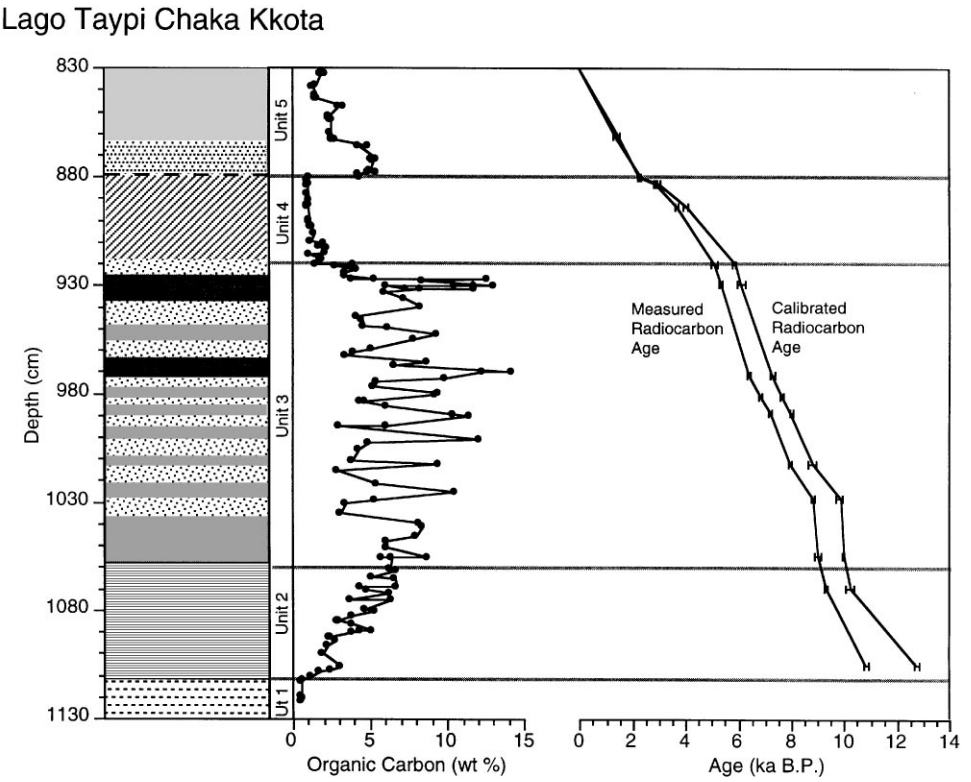


Fig. 2. Core description, OC, and age/depth relationship for both measured and calibrated radiocarbon ages with one sigma error bars.

one sigma error as both measured ($^{14}$C yr B.P.) and calibrated ages (cal $^{14}$C yr B.P.) according to Stuiver et al. (1998), but only cal ages are discussed in the context of the paleo-reconstruction in order to make the LTCK record more directly comparable with ice core and U-series chronologies. All $^{14}$C measurements were made by accelerator mass spectrometry (AMS) at Lawrence Livermore National Laboratories (CAMS). An age-depth model has been constructed by linear interpolation of the fourteen calibrated *Isoetes* $^{14}$C dates (Fig. 2). Hereafter, all ages discussed are calibrated ages (cal $^{14}$C yr B.P. or ka B.P.).

## 4. Results

### 4.1. Modern surface water samples

Oxygen and hydrogen isotope ratios were measured for water samples from 23 lakes collected during the dry winter season along a north to south transect spanning the Cordillera Vilcanota (14° S), Cordillera Real (16° S), Cordillera Tunari (17° S), and Cordillera Chichas (19° S) (Table 1; Fig. 1). Water samples were collected approximately 20 cm below the surface in the center of the lake. These lakes are representative of different hydrologic settings, including: (1) lakes directly receiving glacial meltwater, (2) overflowing lakes in glaciated watersheds, (3) overflowing lakes in watersheds without active glaciers, and (4) lakes and ponds that drop below the overflow level during the dry season. Results show a wide range of isotopic compositions with $\delta^{18}$O varying between $-16.6$ and $-2.5$ and $\delta^{2}$H varying between $-127$ and $-56‰$ (Fig. 3).

### 4.2. Lithology and geochronology

Five lithostratigraphic units have been defined from the LTCK core. These are described in chronological order. These units form the basis on which the other proxies are subsequently presented (Fig. 4).

Unit 1 is characterized as a massive gray section with low OC ($<1\%$), low C/N ratios ($<7$), high silt-sized mineral concentration ($>95\%$), low biogenic silica values ($<5\%$), high bulk density ($>1$ g cm$^{-3}$), and high mass magnetic susceptibility ($1\times10^{5}$ SI) (Fig. 4). The transition from Unit 1 into Unit 2 is identified by a shift from massive silts to finely laminated sediments. The radiocarbon age of the upper surface of the transition from gray silts to organic silts is 12,720 cal $^{14}$C yr B.P. (CAMS-19243) (Table 2). The contact is diffuse (6 cm) and characterized by increased OC concentration from $<1$ to $>3\%$, increased C/N ratio from 6 to 8, increased biogenic silica from $<5$ to $>10\%$, decreased dry bulk

Table 1
Watershed data for lakes where modern water samples were collected

| Lake | Cordillera | Latitude | Longitude | Lake elevation (m) | Headwall elevation (m) | Glaciers present | $\delta^{18}O$ | $\delta^{2}H$ |
|---|---|---|---|---|---|---|---|---|
| Accocanch | Vilcanota | 13° 54′ 00″ S | 70° 54′ 15″ W | 4780 | 5000 | yes | − 15.0 | − 119 |
| Paca Cocha | Vilcanota | 13° 54′ 38″ S | 71° 52′ 42″ W | 4925 | 5000 | yes | − 16.6 | − 124 |
| Churuyo | Vilcanota | 14° 01′ 28″ S | 70° 56′ 07″ W | 4710 | 5000 | yes | − 16.5 | − 127 |
| Ajuyani Sorata | Real | 15° 53′ 43″ S | 68° 35′ 07″ W | 4120 | 4240 | | − 9.5 | − 81 |
| Jankaho | Real | 16° 04′ 25″ S | 68° 19′ 10″ W | 4690 | 5596 | yes | − 15.2 | − 115 |
| Khotia | Real | 16° 06′ 45″ S | 68° 20′ 22″ W | 4460 | 5589 | yes | − 13.1 | − 102 |
| Unnamed Pond | Real | 16° 07′ 40″ S | 68° 21′ 10″ W | 4470 | 4480 | | − 2.5 | − 56 |
| Khara Kkota | Real | 16° 09′ 10″ S | 68° 22′ 08″ W | 4300 | 5589 | yes | − 14.6 | − 109 |
| Allkha Kkota | Real | 16° 08′ 50″ S | 68° 18′ 45″ W | 4510 | 5648 | yes | − 15.8 | − 110 |
| Sora Kkota | Real | 16° 11′ 02″ S | 68° 20′ 40″ W | 4300 | 5650 | yes | − 15.1 | − 114 |
| Taypi Chaka Kkota | Real | 16° 12′ 10″ S | 68° 21′ 08″ W | 4300 | 5650 | yes | − 14.8 | − 112 |
| Ajwani | Real | 16° 10′ 30″ S | 68° 19′ 15″ W | 4550 | 5260 | yes | − 15.2 | − 113 |
| Viscachani | Real | 16° 11′ 32″ S | 68° 07′ 24″ W | 4100 | 5300 | yes | − 14.4 | − 108 |
| Sayto | Tunari | 17° 12′ 24″ S | 66° 22′ 33″ W | 4300 | 4820 | | − 12.9 | − 98 |
| Cupetani | Tunari | 17° 13′ 28″ S | 66° 24′ 42″ W | 4400 | 4820 | | − 12.6 | − 102 |
| Upper San Ignacio | Tunari | 17° 14′ 40″ S | 66° 11′ 28″ W | 4400 | 4580 | | − 12.3 | − 97 |
| San Ignacio Main | Tunari | 17° 14′ 50″ S | 66° 11′ 45″ W | 4380 | 4580 | | − 11.9 | − 97 |
| San Ignacio Pond | Tunari | 17°14′ 52″ S | 66° 11′ 35″ W | 4400 | 4580 | | − 6.1 | − 72 |
| Mosoj | Tunari | 17° 16′ 22″ S | 66° 00′ 40″ W | 4270 | 4204 | | − 9.2 | − 82 |
| Huallancani | Tunari | 17° 17′ 07″ S | 66° 00′ 50″ W | 4250 | 4204 | | − 10.5 | − 88 |
| Juntutuyo | Tunari | 17° 33′ 34″ S | 65° 39′ 34″ W | 3380 | 3922 | | − 4.9 | − 57 |
| Potosi #1 | Chichas | 19° 38′ 20″ S | 65° 41′ 50″ W | 4640 | 5024 | | − 5.6 | − 59 |

density from $>1$ to $<0.6$ g cm$^{-3}$, and decreased mass magnetic susceptibility from $>1\times10^{5}$ to $<0.5\times10^{5}$ SI.

Unit 2 spans the time interval from 12.7 to 10.0 ka B.P. and is a finely laminated (mm-scale) brown section with contrast between layers alternating between faint and clear. Unlike Unit 1, this section has a clear trend from the base to the top characterized by increasing OC concentration from $<1$ to $>8$%, increasing C/N ratio from $\sim7$ to $\sim10$, a decreasing trend in the mineral concentration from $>90$ to $<40$%, increasing biogenic silica from $<5$ to $>40$%, decreasing dry bulk density from $>1$ to $<0.5$ g cm$^{-3}$, and decreasing mass magnetic susceptibility from $>1\times10^{5}$ to $<0.5\times10^{5}$ SI (Fig. 4). The transition from Unit 2 into Unit 3 occurs at 9970 cal $^{14}$C yr B.P. (CAMS–10033) and is marked by a change from finely laminated (mm-scale) to banded (cm-scale) sediments alternating between light ($<5$% OC) and dark layers (10% OC). The contact into the first light band at the base of Unit 3 is abrupt (1 cm) and characterized by decreased OC concentration from $>8$ to $<4$%, increased C/N ratio from 9 to 10, increased biogenic silica from $<40$ to $>50$%, and little change in the already very low values of dry bulk density and mass magnetic susceptibility.

Unit 3 spans the time interval from 10.0 to 6.0 ka B.P. Unit 3 is characterized by alternating centimeter-scale bands of high ($>10$%) and low ($<5$% and lower) OC concentration, variable C/N ratios ranging between 9 and 13 with a slight increasing trend from the base to the top, variable mineral concentration ranging from 20 to $>75$%, high biogenic silica (generally $>40$%), low bulk density ($<0.4$ g cm$^{-3}$), and low mass magnetic susceptibility ($<0.4\times10^{5}$ SI) (Fig. 4). The dark brown organic-rich bands contain abundant *Isoetes* megaspores. There is not a systematic change in C/N ratio, mineral concentration, or biogenic silica between the light and dark bands, nor is there a significant shift in the diatom composition or lipid biomarkers in the light and dark bands (Polissar, 1999). The transition from Unit 3 into Unit 4 is identified by a change from banded (cm-scale) sediments alternating between light and dark layers to a massive unit with low OC. The radiocarbon age of the lower surface of the transition from banded organic-rich sediments to massive gray silts is 5900 cal $^{14}$C yr B.P. (CAMS-5748). The contact is diffuse (7 cm) and characterized by decreased OC concentration from $>10$ to $<2$%, decreased C/N ratio from $>10$ to $<8$, no significant change in biogenic silica, increased dry bulk density from 0.4 to $>0.5$ g cm$^{-3}$, and increased mass magnetic susceptibility from 0.5 to 0.6x10$^{5}$ SI.

Unit 4 spans the time interval from 6.0 to 2.3 ka B.P. Unit 4 is a massive gray section characterized by low OC concentration ($<2$%), a trend toward lower C/N ratios from $\sim10$ to $\sim6$ falling at the base of the unit, an increasing trend in the mineral concentration from 40 to $>65$%, a decreasing trend in biogenic silica from $\sim50$ to $\sim30$% beginning at the mid-point of the unit, an increasing trend in dry bulk density from $\sim0.4$ to

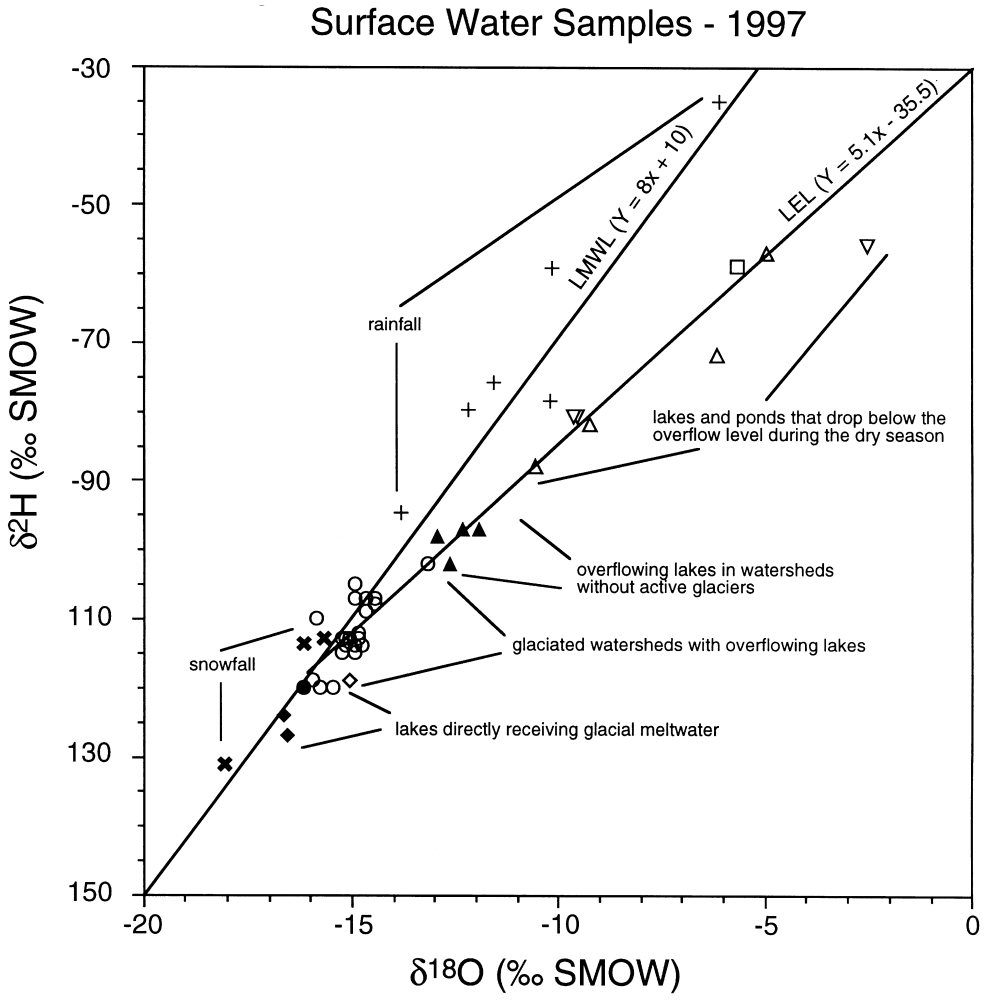


Fig. 3. Results of $\delta^2H$ and $\delta^{18}O$ measurements from lake waters collected during the 1997 field season in the Bolivian Andes showing: (1) lakes directly receiving glacial meltwater plot on the MWL or just off and have essentially the same $\delta^2H$ and $\delta^{18}O$ values as snow (◆ Cordillera Vilcanota and ● Cordillera Real), (2) overflowing lakes in glaciated watersheds are generally more $^{18}O$-enriched than glacial-fed lakes (◇ Cordillera Vilcanota and ○ Cordillera Real), (3) overflowing lakes in watersheds without active glaciers are further $^{18}O$-enriched (▲ Cordillera Tunari), (4) lakes and ponds that drop below the overflow level during the dry season are the most $^{18}O$-enriched of the lakes sampled (▼ Cordillera Real, △ Cordillera Tunari, and □ Cordillera Chichas). Rainfall ( + ) and snowfall (×) plot along the Meteoric Water Line (MWL) (Stimson, 1991).

$> 0.8$ g cm$^{-3}$, and an abrupt increase in mass magnetic susceptibility from $< 0.4 \times 10^5$ $> 1.5 \times 10^5$ SI at the midpoint of the unit (Fig. 4). The transition from Unit 4 into 5 is marked by an abrupt change in the sediment character from massive gray silts to organic silts and radiocarbon age from 2970 cal $^{14}C$ yr B.P. (CAMS-5749) to 2330 cal $^{14}C$ yr B.P. (CAMS-11067). Marked changes include an increased OC from $< 1$ to $> 5\%$, increased C/N ratio from values averaging 6.8–8.0, increased biogenic silica from $\sim 20$ to $\sim 30\%$, decreased dry bulk density from 0.8 to 0.4 g cm$^{-3}$, and decreased mass magnetic susceptibility from $> 1.5 \times 10^5$ to $< 0.4 \times 10^5$ SI.

Unit 5 spans the time interval from 2.3 ka B.P. to the present. Unit 5 is a massive unit with a gradual change in color from brown to gray at the surface. This unit is characterized by a decreasing trend in OC concentration up-core, C/N ratios between 7 and 8, an increasing trend in the mineral concentration from 50 to $> 90\%$, a decreasing trend in biogenic silica from $> 30$ to $< 5\%$, an increasing trend in dry bulk density from $< 0.4 > 0.7$ g cm$^{-3}$, and an increasing trend in mass magnetic susceptibility from $< 0.4 \times 10^5$ to $> 1.5 \times 10^5$ SI) (Fig. 4). A radiocarbon age of 1340 cal $^{14}C$ yr B.P. (CAMS-4980) dates the point above which mineral concentration comprises $> 90\%$ of the sediment.

### 4.3. $\delta^{18}O_{lw}$

Unit 1 is characterized by low $\delta^{18}O_{lw}$ values of $< -14‰$ (Fig. 5). The transition from Unit 1 into Unit 2 is marked by a 3‰ increase in $\delta^{18}O_{lw}$ from $-14$ to $-11‰$. Unit 2 shows clear trends from the base to the

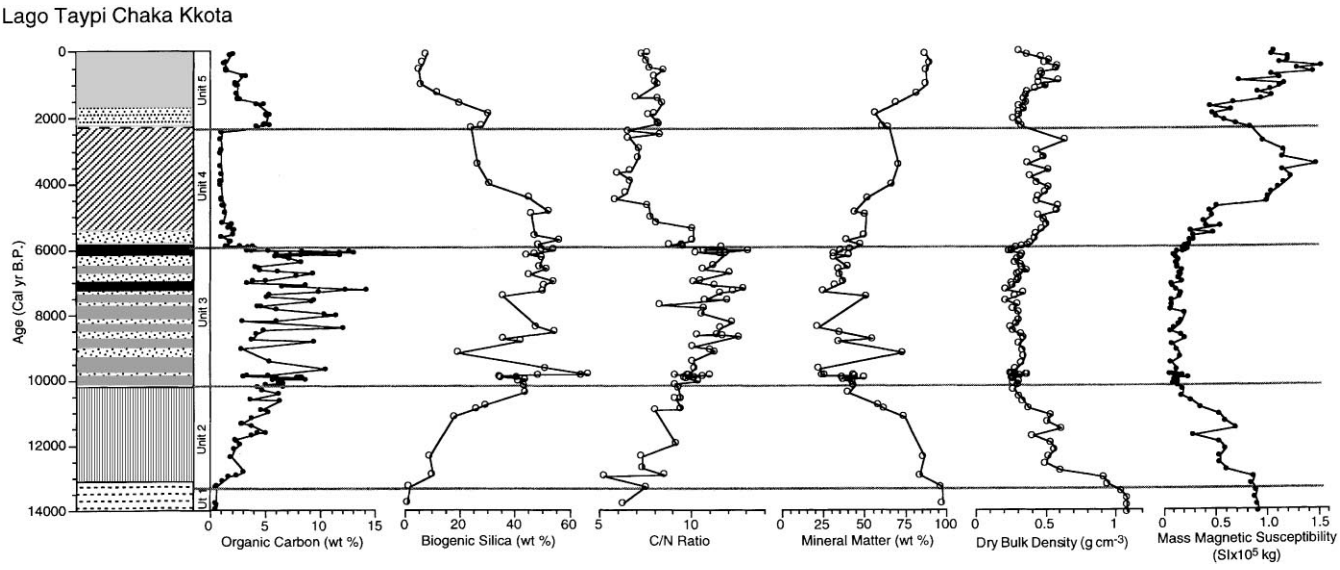


Fig. 4. Core data plotted on an age scale including OC, biogenic silica, C/N ratio, mineral matter, dry bulk density, and mass magnetic susceptibility.

Table 2
Radiocarbon ages from LTCK, Bolivia

| CAMS-# | Depth (cm) | Material | Measured $^{14}$C Age ($^{14}$C yr B.P.) | Median calibrated $^{14}$C Age (Cal $^{14}$C yr B.P.) |
|---|---|---|---|---|
| 4980 | 860.5 | *Isoetes* macrofossil | 1470 ± 80 | 1340 |
| 11067 | 879.5 | *Isoetes* macrofossil | 2290 ± 60 | 2330 |
| 11068 | 882.5 | *Isoetes* macrofossil | 2880 ± 60 | 2970 |
| 5749 | 893.5 | *Isoetes* macrofossil | 3690 ± 70 | 4040 |
| 5748 | 919.5 | *Isoetes* macrofossil | 5110 ± 60 | 5900 |
| 4979 | 928.5 | *Isoetes* macrofossil | 5320 ± 110 | 6100 |
| 10031 | 971 | *Isoetes* macrofossil | 6390 ± 60 | 7260 |
| 10032 | 981 | *Isoetes* macrofossil | 6840 ± 60 | 7630 |
| 10063 | 988.5 | *Isoetes* macrofossil | 7210 ± 70 | 7960 |
| 10066 | 1011.5 | *Isoetes* macrofossil | 7960 ± 60 | 8810 |
| 10065 | 1028 | *Isoetes* macrofossil | 8810 ± 110 | 9860 |
| 10033 | 1054 | *Isoetes* macrofossil | 8980 ± 70 | 9970 |
| 10064 | 1069.5 | *Isoetes* macrofossil | 9300 ± 100 | 10240 |
| 19243 | 1104.5 | *Isoetes* macrofossil | 10790 ± 60 | 12720 |

top characterized by an increase in $\delta^{18}O_{lw}$ from $\sim -12$ to $\sim -9‰$. The transition from Unit 2 into Unit 3 is marked by a 6‰ decrease in $\delta^{18}O_{lw}$ from $-8$ to $-14‰$. Unit 3 is characterized by relatively low $\delta^{18}O_{lw}$ values ranging from $-16$ to $-11‰$ with no systematic change in the values of the $\delta^{18}O_{lw}$ between light and dark bands. The transition from Unit 3 into Unit 4 is characterized by a $\sim 5‰$ increase in $\delta^{18}O_{lw}$ from $-13$ to $-8‰$. Unit 4 has variable but generally high $\delta^{18}O_{lw}$ values ranging from $-14$ to $-4‰$. The transition from Unit 4 into Unit 5 is marked by an abrupt change in the sediment character and radiocarbon age from 2970 to 2330 cal $^{14}$C yr B.P. This boundary is marked by a 5.3‰ decrease in $\delta^{18}O_{lw}$. Unit 5 is characterized by relatively low $\delta^{18}O_{lw}$ values ranging from $-14.3‰$ at the surface to $-10‰$.

### 4.4. $\delta^{13}C_{cell}$ *and* $\delta^{13}C_{org}$

Generally, measurements of $\delta^{13}C_{org}$ and $\delta^{13}C_{cell}$ from the same interval are correlated and $\delta^{13}C_{org}$ values are less than $\delta^{13}C_{cell}$ values (Fig. 5). Unit 1 is characterized moderate $\delta^{13}C$ values for both $\delta^{13}C_{cell}$ ($-22.5‰$) and $\delta^{13}C_{org}$ ($-22.8‰$). The transition from Unit 1 into Unit 2 is identified by a slight decrease of $< 1‰$ in both $\delta^{13}C_{cell}$ and $\delta^{13}C_{org}$. Unit 2 shows clear trends from the base to the top characterized by a slight increase of about 1‰ for both $\delta^{13}C_{cell}$ and $\delta^{13}C_{org}$. The transition from

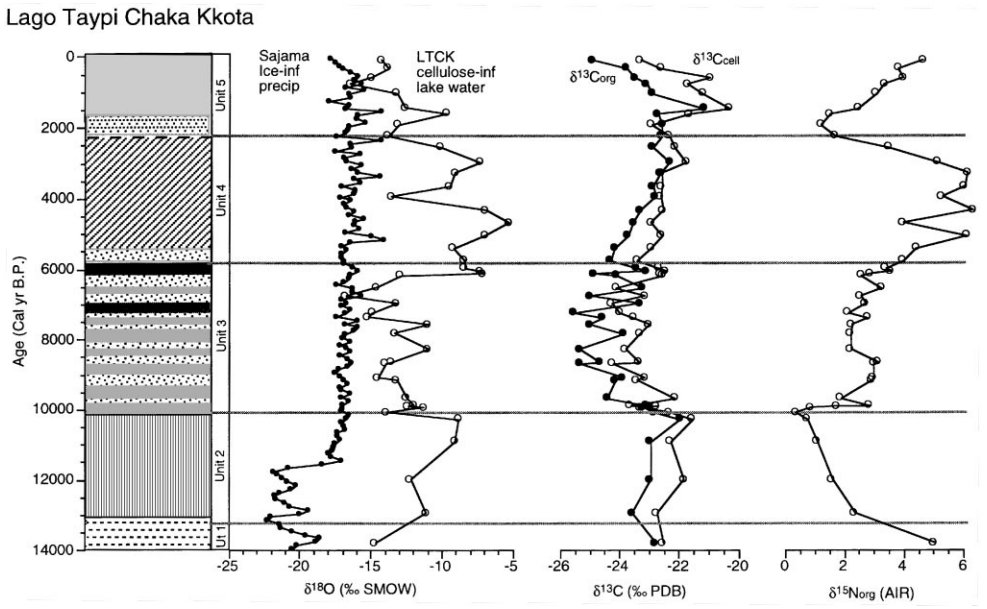


Fig. 5. Stable isotope data plotted on an age scale including cellulose inferred $\delta^{18}O_{lw}$, $\delta^{13}C_{cell}$ and $\delta^{13}C_{org}$, and $\delta^{15}N_{org}$.

Unit 2 into Unit 3 is identified by a slight decrease of $< 1‰$ in both $\delta^{13}C_{cell}$ and $\delta^{13}C_{org}$. Unit 3 is characterized by alternating light and dark centimeter-scale bands of high (10% and greater) and low (5% and lower) OC concentration. The $\delta^{13}C_{cell}$ and $\delta^{13}C_{org}$ values are highly variable ranging from $-26$ to $-23‰$ with sediment cellulose generally being higher. The transition from Unit 3 into Unit 4 is identified by a slight decrease of $< 1\%$ in both $\delta^{13}C_{cell}$ and $\delta^{13}C_{org}$. Unit 4 is a massive section characterized by both $\delta^{13}C_{cell}$ and $\delta^{13}C_{org}$ increasing from $-25$ to $-22‰$ with sediment cellulose being higher by approximately 1‰. Although $\delta^{13}C$ values do not change abruptly across the transition from Unit 4 into 5 both $\delta^{13}C_{cell}$ and $\delta^{13}C_{org}$ become increasingly lower through time and the difference between sediment cellulose and bulk sediment increases at the top of the core. $\delta^{13}C$ values increase in the lower strata of Unit 5 and then decrease towards the top of the core.

### 4.5. $\delta^{15}N_{org}$

Bulk sediment $\delta^{15}N$ varies between values of 0 and 5.4‰ during the Holocene (Fig. 5). Unit 1 is characterized by a high $\delta^{15}N_{org}$ value of $> 5‰$. The transition from Unit 1 into 2 is marked by a shift to lower $\delta^{15}N_{org}$ values ranging from $> 5$ to $< 3‰$. Unit 2 has a clear trend from the base to the top towards lower $\delta^{15}N_{org}$ values ranging for from $> 3$ to $0‰$. The transition from Unit 2 into Unit 3 is identified by an abrupt increase from 0 to $> 2‰$. Unit 3 is characterized by alternating dark and light centimeter-scale bands of high ($> 10\%$) and low ($< 5\%$) OC concentration. After an initial trend toward higher $\delta^{15}N_{org}$ values from 0 to $> 3‰$ values remain relatively constant ranging from 2 to 3‰. The transition from Unit 3 into Unit 4 is identified by an increase from 3.0 to 4.5‰. Unit 4 is massive section characterized by a trend toward higher $\delta^{15}N_{org}$ values ranging from $\sim 4$ to $\sim 5‰$. The transition from Unit 4 into Unit 5 is marked by a $> 3‰$ decrease in $\delta^{15}N_{org}$ from values averaging 5 to 2‰. Unit 5 is characterized by a trend toward higher $\delta^{15}N_{org}$ values from $< 1$ to $> 5‰$.

### 4.6. Diatoms

The diatom flora in the sediments of LTCK totals 76 identified taxa (Appendix A). Fig. 6 shows the relative frequencies of the 15 most abundant taxa that amount to $> 82\%$ of any one sample. Four broad diatom stratigraphic zones are identified. Although the four diatom stratigraphic zones broadly correlate to the five litho stratigraphic zones defined above there are notable differences. While the transitions from a glaciated watershed to a non-glaciated catchment and back occur at approximately the same time in both the diatom and litho stratigraphic units, the middle Holocene period of seasonal desiccation identified in the lithostratigraphic units, record does not appear as clearly in the diatom record. Perhaps this is because the lake desiccated periodically throughout the early to middle Holocene.

The diatom record begins in the uppermost portion of sediment Unit 1, with a flora characterized by small colonial *Fragilaria* spp. and *Aulacoseira alpigena* (diatom zone 1). This assemblage persists until $\sim 11$ ka B.P., at which time larger benthic taxa become dominant

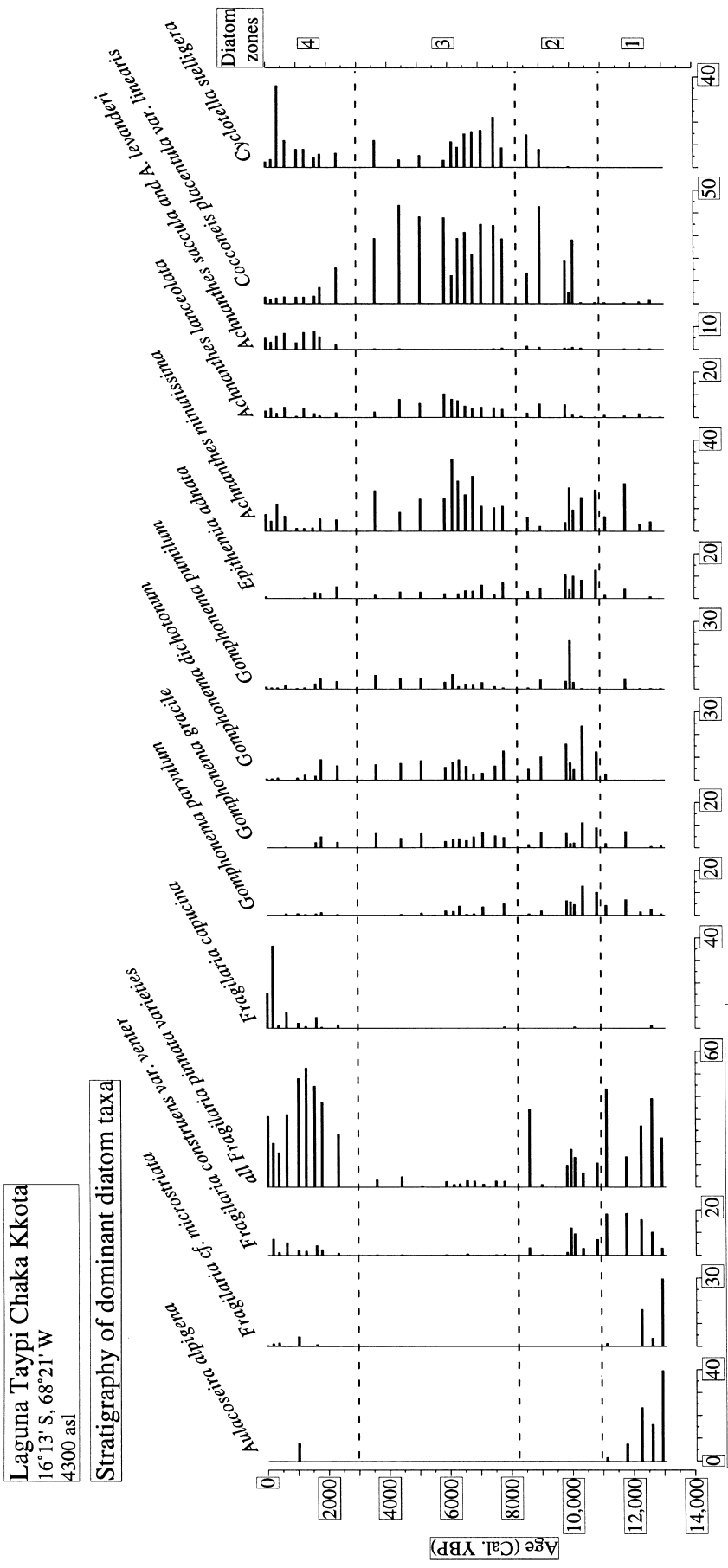


Fig. 6. Stratigraphic sequence of the relative frequencies of the 15 most abundant diatom taxa in the LTCK core, arranged according to the age model of Fig. 2. The four biostratigraphic zones discussed in the text are defined to the right.

co-occurrent diatoms, including several *Gomphonema spp*., *Cocconeis placentula* var. *linearis*, and *Epithemia adnata* (diatom zone 2). These mostly periphytic diatoms, in addition to several *Achnanthes* spp. and *Cyclotella stelligera*, become increasingly dominant after 8 ka B.P. (diatom zone 3), after which time *Fragilaria* spp. are only minor components of assemblages ( $< 10\%$). However, by 2.5 ka B.P. and throughout sediment Unit 5, the *Fragilaria* association regains importance, so that diatom zone 4 bears some resemblance to zone 1, with the exceptions of relatively high frequencies of *C. stelligera* and small *Achnanthes* spp. in the former.

Diatom valve concentrations in the sediments of LTCK exceed $10^8$ valves $cm^{-3}$ and are highest in diatom zones 2 and 3. This trend corresponds well with the biogenic silica concentration of the sediments (Fig. 7 A and B). Biogenic silica decreases more dramatically at the base and top of the core relative to diatom concentrations; this is related to the small size of diatoms in these portions of the core. Together, the absolute diatom abundance and biogenic silica trends suggest suppressed diatom production during the late Pleistocene and the late Holocene. The first two axes of Detrended Correspondence Analysis account for 31.4% and 9.9% of the variance in the assemblage data. Only axis 1 results are shown (Fig. 7C and D). Diatom assemblages with high DCA axis 1 scores characterize diatom zones 1 and 4, due to high proportions of taxa such as *Fragilaria* and *Achnanthes spp*., and *Aulacoseira alpigena* (Fig. 7D). Samples with the lowest DCA axis 1 scores are in zone 3, where large periphytic taxa and *Cyclotella stelligera* dominate assemblages.

## 5. Discussion

### 5.1. Isotopic composition of modern lake water

Lake-water samples diverge from the local meteoric water line (LMWL) as a result of the extent of evaporative enrichment of $^{18}O$ and $^{2}H$ (Fig. 3) (cf. Aravena et al., 1999). Lakes fed directly by glacial meltwater are the most depleted in $^{18}O$ and $^{2}H$ because water rapidly passes through these basins without much evaporation. On the other end, of the spectrum, lakes and ponds that annually drop below the overflow level during the dry season are the most enriched in $^{18}O$ and $^{2}H$. The slope of the local evaporation line (LEL $= 5.1$), which is primarily a function of relative humidity (Gonfiantini, 1986), is similar to that of surface waters from closed basins elsewhere on the Bolivian and Chilean altiplano (Fritz et al., 1981). The estimated mean annual isotopic composition of precipitation for this region is $-16‰$ for $\delta^{18}O$ and $-118‰$ for $\delta^{2}H$ as determined from the interception of the LEL and LMWL. These values are typical for glacial meltwater and groundwater above an altitude of 4000 m in the altiplano region (Stimson, 1991; Stimson et al., 1993; Coudrain-Ribstein et al., 1995).

The $\delta^{18}O$ and $\delta^{2}H$ data from our sampling network indicate that lakes in the region are sensitive to variations in P–E balance. This sensitivity is highlighted when a lake and associated catchment undergo a climatically induced change in status, such as going from a glaciated to a non-glaciated watershed or from an overflowing lake to a system that drops below the overflow level on an annual basis. Lake depth, lake area, watershed area, and

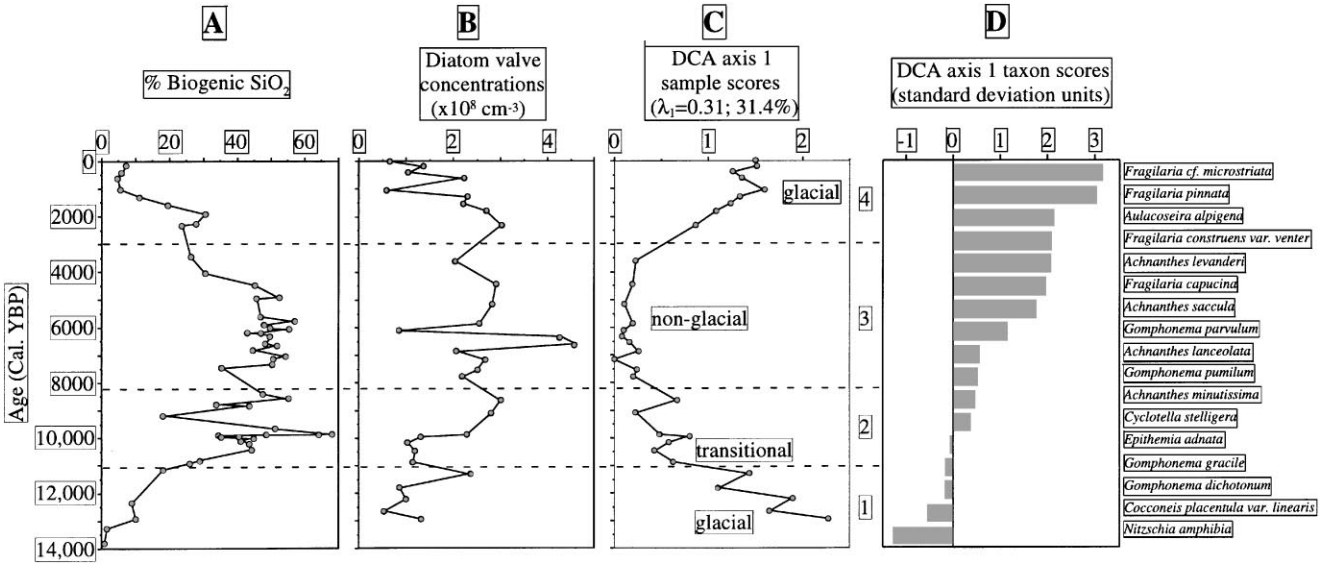


Fig. 7. (A) Weight percent biogenic silica; (B) diatom valve concentrations; (C) fossil sample scores on the first axis of a (detrended) Correspondence Analysis ordination, distinguishing lacustrine paleoenvironments according to the diatom zones illustrated in Fig. 6; and (D) taxon scores from this ordination exercise. Taxa with the highest (positive) scores in (D) are associated with glacial conditions, whereas lower scores indicate mostly periphytic taxa associated with lower water levels and at least occasional evaporative conditions.

the presence or absence of glaciers in the catchment are factors that influence lake water isotopic composition, but more intensive site-specific sampling is required to fully evaluate these effects. These preliminary data nonetheless provide a useful context to identify lakes that are today sensitive to P–E changes and to aid in the interpretation of down-core cellulose $\delta^{18}O$ measurements to evaluate the paleohydrology of the lake basin.

### 5.2. Origin of sediment organic matter

A prerequisite for reconstructing $\delta^{18}O_{lw}$ history from cellulose $\delta^{18}O$ is that the fine-grained cellulose fraction must be derived from an aquatic source. Both elemental and isotopic evidence suggest that this is the case for the LTCK sediments. The C/N ratio of bulk organic samples from the sediment core range between 6 and 13 (Fig. 4), consistent with values measured on modern submerged aquatic vegetation from the lake ($11.4 \pm 3.6$; Table 3). The C/N ratios are higher for samples of *Isoetes* ($17.8 \pm 5.0$) that were collected along the margin of the lake which is exposed to subaerial conditions during the dry season. The C/N ratio for modern terrestrial vegetation average $33.3 \pm 18.6$, which is considerably higher than those of aquatic plants.

Cellulose-inferred $\delta^{18}O_{lw}$ values obtained from the uppermost sediments of the LTCK core ($-14.3‰$) and modern submerged aquatic vegetation, green algae ($-13.5‰$) and *Myriophyllum* ($-14.1‰$), correspond well with the measured lake water $\delta^{18}O$ value of $-14.8‰$ (Tables 1 and 4). The agreement suggests that the observed cellulose-water oxygen isotope fractionation factor of $1.028 \pm 0.001$ applies not only to temperate and Arctic aquatic cellulose (e.g. Edwards and McAndrews, 1989; Duthie et al., 1996; Edwards et al., 1996; Wolfe and Edwards, 1997), but also to tropical aquatic cellulose in alpine settings, even though others have used a smaller fractionation factor (Aucour et al., 1993; Beuning et al., 1997). The higher cellulose-inferred $\delta^{18}O_{lw}$ value obtained from *Isoetes* ($-10.7‰$; Table 4) is likely due to additional isotopic enrichment caused by evapotranspiration, because this sample was collected from the margin of the lake zone where the plant is not continuously submerged during the dry season. The effects of evapotranspiration are also clearly evident in the cellulose $\delta^{18}O$ value of $+21.9‰$ determined on puna grass, a terrestrial plant (Table 4). Given the limitations of this small data set, green algae appears to be a significant source of organic matter to the offshore $< 500$ μm fraction in at least the most recent lake sediments, given the strongly $^{13}C$-enriched signature of *Myriophyllum* relative to the surface sediments (Table 4).

Table 3
C/N ratios and stable isotope composition of modern vegetation and surface sediments sampled in 1994 and analyzed at the University of Alaska at that time

| Initial Data | Number of samples | C/N | $\delta^{13}C$ | $\delta^{15}N$ |
|---|---|---|---|---|
| Aquatic vegetation | 12 | $11.4 \pm 3.6$ | $-24.53 \pm 2.20$ | $4.87 \pm 1.63$ |
| Shoreline vegetation (*Isoetes*) | 3 | $17.8 \pm 5.0$ | $-26.58 \pm 0.52$ | $4.05 \pm 1.19$ |
| Terrestrial vegetation | 12 | $33.3 \pm 18.6$ | $-27.51 \pm 1.33$ | $2.16 \pm 2.17$ |
| Surface Sediment | 4 | $10.7 \pm 0.6$ | $-24.85 \pm 0.22$ | $6.57 \pm 0.35$ |

Table 4
C/N ratios and stable isotope composition of modern vegetation and surface sediments sampled in 1997 and analyzed at the University of Waterloo. Cellulose-inferred lake-water $\delta^{18}O$ values (cell-inf. $\delta^{18}O_{lw}$) calculated using a cellulose–water oxygen isotope fractionation factor of 1.028

| | C/N | $\delta^{18}C$ | $\delta^{15}N$ | $\delta^{18}O_{cell}$ | cell-inf.$\delta^{18}O_{lw}$ |
|---|---|---|---|---|---|
| Aquatic: | | | | | |
| Green algae | 12.3 | −22.47 | 5.11 | 14.2 | −13.5 |
| *Myriophyllum* | 10.5 | −11.76 | 5.71 | 13.5 | −14.1 |
| *Isoetes* | 42.4 | −22.93 | 3.71 | 17.1 | −10.7 |
| Terrestria: | | | | | |
| Puna grass | 188.8 | −24.85 | 1.19 | 21.9 | — |
| Core: | | | | | |
| Top sediments | 7.6 | −24.93 | 4.69 | 13.3 | −14.3 |

### 5.3. Late-glacial and holocene paleohydrology

If we assume an aquatic source for the fine-grained cellulose for the whole length of the LTCK sediment record, further interpretation of the $\delta^{18}O_{lw}$ profile requires separating the isotopic composition of water supplied to the lake integrating the isotopic signature of surface water, groundwater, and precipitation from hydrologic factors that subsequently modify the isotopic ratio, primarily evaporative enrichment. To investigate the long-term oxygen isotope history of precipitation ($\delta^{18}O_p$) in the region we compared the data from LTCK with the ice core $\delta^{18}O$ record for the past 15 ka B.P. obtained from Nevado Sajama (Thompson et al., 1998), located on the western edge of Bolivian altiplano (18°06′S, 68°53′W, 6542 m; Fig. 1).

The Sajama ice core record shows a rapid $^{18}O$-depletion of about $6‰$ from $-15$ to $-21‰$ at 14 ka B.P. Thompson et al. (1998) interpret this trend as a change from a warm-dry period, culminating at 14.3 ka B.P., to a cold–wet phase similar to the North Atlantic Younger Dryas. However, the $> 2.5$ m of inorganic sediments in LTCK Unit 1 (deposited prior to 12.7 ka B.P. and not

shown in the figures) are dominated by silt-sized mineral matter typical of modern glacier-fed lakes in the Cordillera Real, suggesting that the watershed was undergoing deglaciation. The single $^{18}O$-depleted lake-water value of $-14.7\%$ from this interval is consistent with modern lakes that are overflowing and have glaciers in the watershed (Fig. 3). Likewise, the sparse diatom assemblages dominated by *Aulacoseira alpigena* and *Fragilaria* spp are also similar to the modern lake sediment which is influenced by active glaciers in the catchment. Rapid deglaciation beginning prior to 13.8 ka B.P. is also documented in three other lakes from our regional study spanning the latitudes of 16°S to 20°S (Lagunas Ajuyani, San Ignacio, and Potosí) and in several other studies along the eastern Cordillera (Mercer and Palacios, 1978; Seltzer, 1990, 1992). The evidence provided for regional deglaciation is inconsistent with the deglacial climatic reversal proposed by Thompson et al. (1998) spanning the period between $\sim 14.0$ and 11.5 ka B.P. Modeling studies by Hostetler and Giorgi (1992) illustrated the impact a large pluvial lake system has on regional climate. We speculate one possible explanation for the decrease in $\delta^{18}O$ values in the ice core may be in part the result of local dilution of atmospheric precipitation with $^{18}O$-depleted vapor derived from the formation of pluvial lakes on the altiplano during deglaciation in the eastern cordillera.

The beginning of the Holocene in the Sajama ice core is marked by an enrichment in $^{18}O$ of 4 to about $-17\%$ at 11.5 ka B.P. suggesting either rapid warming (Thompson et al., 1998) or the draw-down of pluvial lakes on the altiplano that had previously been a major source for isotopically light precipitation. LTCK Unit 2 sediments (13.1 and 10 ka B.P.) are characterized by higher OC and biogenic silica concentration (Fig. 4) consistent with increased lacustrine productivity as glaciers retreated up valley, reduced meltwater influx, and stabilized slopes with the establishment of terrestrial vegetation (Abbott et al., 1997a). Although the diatom taxa typical of glacially influenced limnological conditions are present throughout Unit 2, the flora begins to diversify after 11 ka B.P., suggesting progressive ecological changes during the transition towards non-glacial conditions (Fig. 7). The increase in cellulose-inferred lake water $\delta^{18}O$ values from $-12.2$ to $-8.2\%$ between 11.9 and 10.9 ka B.P. may therefore reflect drier conditions and increased evaporation associated with late Pleistocene – early Holocene warming and/or a reduction in glacial meltwater supply due to warming and increased aridity.

Ice core $\delta^{18}O$ values from the Sajama ice core remain at about $-17 \pm 1‰$ during the Holocene (Fig. 8), similar to modern mean annual $\delta^{18}O_p$ (Fig. 4). Evidently, climatic variation during the Holocene is not strongly reflected in centennial-scale $\delta^{18}O_p$ as recorded in the Sajama ice core record. This suggests that variations in the Holocene LTCK $\delta^{18}O_{lw}$ record are largely decoupled from changes in $\delta^{18}O_p$ and supports our interpretation that the observed shifts in $\delta^{18}O_{lw}$ are primarily driven by evaporative enrichment and not a shift in the source of the precipitation.

After 10.9 ka B.P., $\delta^{18}O_{lw}$ returns to lower values characteristic of glacier-fed lakes and remains relatively depleted in $^{18}O$ until 6 ka B.P. (the duration of Unit 3). However, sedimentological evidence suggests that lake-level was variable with multi-decadal to century-scale periods of low water -levels resulting from a general trend of increased aridity that began in the early Holocene (Abbott et al., 1997a). Diatom assemblages are transitional until 8.5 ka B.P. and then are dominated by shallow-water periphytic forms that are not associated with proglacial conditions (Figs. 6 and 7). The diatom data support the sedimentological data, collectively suggesting that glaciers were absent from the watershed during this interval. Several possible explanations can account for the apparent discrepancy between the $^{18}O$-depleted results and data from other proxies. First, C/N ratios increase during this interval, possibly suggesting an increase in the contribution of terrestrial organic matter to the lake. However, modern $\delta^{18}O$ data from a major potential terrestrial source, puna grass, is enriched in $^{18}O$ relative to aquatic sources of organic matter (Table 3) and its isotopic signature would likely have been even higher during this arid interval because of increased evapotranspiration. Second, melting of relic ice from shrinking cirque and rock glaciers may have contributed isotopically light meltwater to LTCK. Although, this most certainly occurred for some period following regional deglaciation, it seems unlikely that this can entirely explain the isotopically low $\delta^{18}O$ values enduring for 4000 years. Third, the relative contribution of snowmelt depleted in $^{18}O$ to LTCK increased relative to summer rainfall, as a result of increased melting, even though the total annual precipitation declined. The snowpack may have melted completely on a seasonal basis during this interval and stored as groundwater, offsetting the isotopic effects of evaporative enrichment of lake water in LTCK, given that seasonal variations in precipitation $\delta^{18}O$ presently vary by more than 16% (Thompson et al., 1998).

Between 6.2 and 2.3 ka B.P., sedimentological evidence indicates LTCK Unit 4 was deposited in a shallow lake that desiccated seasonally (Abbott et al., 1997a). The diatom content of these sediments continues to be dominated by shallow-water non-glacial periphytic taxa (Fig. 6). Subaerial exposure resulted in the oxidation of organic matter and produced a marked unconformity between 2.9 and 2.3 ka B.P. Cellulose-inferred $\delta^{18}O_{lw}$ values are variable, but relatively high during most of this interval, averaging $-8.4‰$. This is within the range of modern lakes that drop to below their overflow levels during the dry season (Fig. 3). Both groundwater and catchment-derived inputs to the lake were likely reduced.

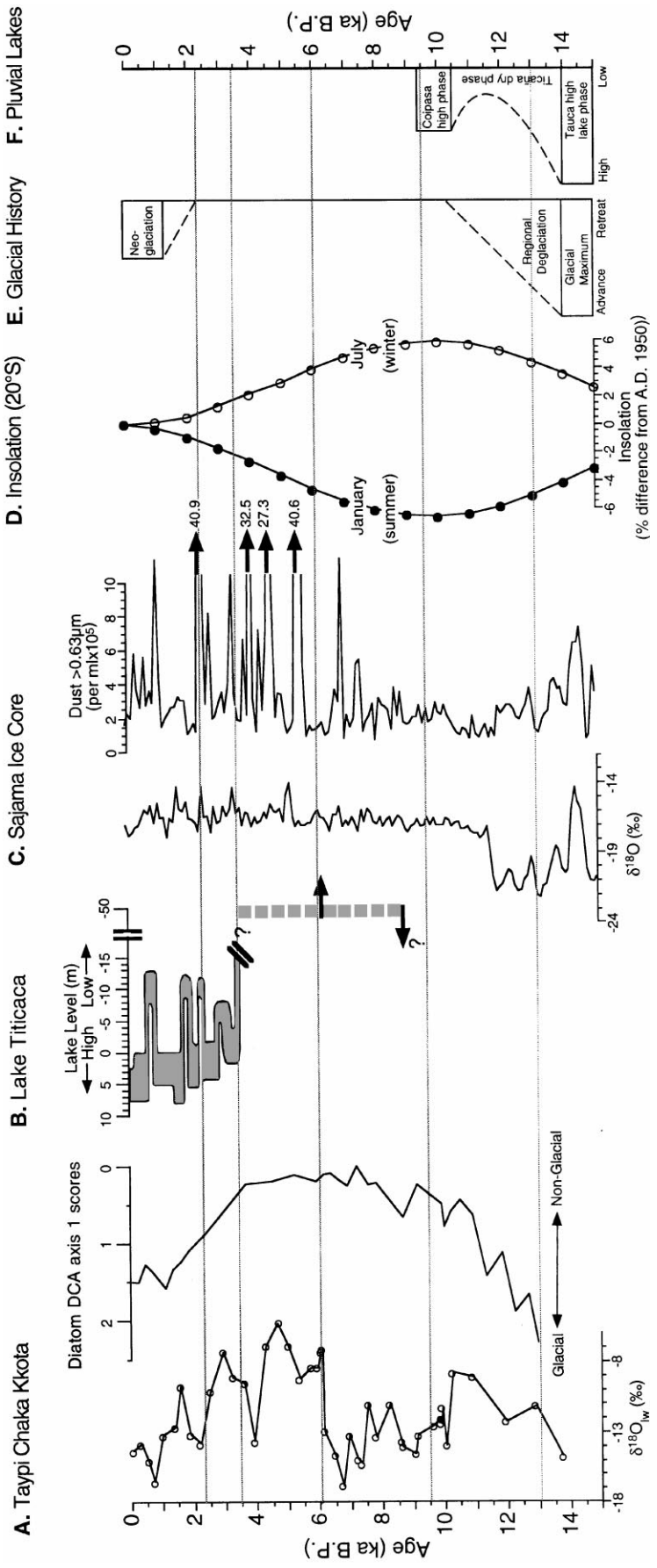


Fig. 8. Summary diagram comparing: (A) the $\delta^{18}O_{lw}$ and diatom DCA showing glacial vs. non-glacial conditions from the LTCK record, (B) water-level fluctuations in Lake Titicaca (Wirrmann and De Oliveira Almeida, 1987; Wirrmann et al., 1992; Wirrmann and Mourguiart, 1995; Abbott et al., 1997b; Mourguiart et al., 1998), (C) the $\delta^{18}O$ and dust records from Nevado Sajama (Thompson et al., 1998), (D) January and July insolation at 20°S (Berger, 1978a, b; Berger and Loutre, 1991), (E) glacial history (Seltzer, 1990, 1992), and (F) pluvial lakes (Servant and Fontes, 1978; Grosjean, 1994; Grosjean et al., 1995; Clayton and Clapperton, 1997). Radiocarbon ages from previous studies were calibrated to calendar years for comparison of time scales.

Snowmelt influxes may have also declined substantially at this time, contributing to strong $^{18}O$-enrichment in the lake sediment cellulose record. Lake water $^{18}O$-enrichment precedes the decline in OC near the transition from Unit 3 to Unit 4 by about 300 yr (Figs. 4 and 5), indicating that during the initial stages of this most arid interval lake level may have dropped, but did not completely desiccate on a seasonal basis. A single $^{18}O$-depleted value of $-13.6\%$ around 3.9 ka B.P. may suggest an episode of reduced aridity or increased snowmelt influx spanning a century or less.

After 2.3 ka B.P., sediments of LTCK Unit 5 show a marked increase in organic matter concentration (Fig. 4) suggesting that LTCK rose to the overflow level. An increase in mineral matter beginning in the lower strata of Unit 5 and culminating at 1.4 ka B.P. suggests the onset of glaciation in the LTCK watershed began at 2.3 ka B.P. and probably reached modern conditions around 1.4 ka B.P. (Fig. 4). Several of the diatom taxa that characterized late-glacial sediments regain importance by 2.3 ka B.P., underscoring an overall floristic similarity between late-glacial and late Holocene assemblages, both of which are associated with glacial inflow to the lake. Values of $\delta^{18}O_{lw}$ average $-13.5\%$ during this interval (Fig. 5), consistent with the return of glacial meltwater influx.

### 5.4. Paleohydrological influence on lake carbon and nitrogen cycling

Systematic variations in $\delta^{13}C_{org}$, $\delta^{13}C_{cell}$ and $\delta^{15}N_{org}$ conform to the stratigraphic units of LTCK (Fig. 5) suggesting a strong linkage between these isotopic signatures, nutrient cycling, and hydrological conditions. Although interpretation of these records is necessarily speculative, given the many factors and processes that can contribute to carbon and nitrogen isotope trends in lake sediments (see Collister and Hayes, 1991; Talbot and Johannessen, 1992; Hodell and Schelske, 1998; Wolfe et al., 1999), reconstruction of the LTCK carbon and nitrogen cycling can be partially constrained within the paleohydrological framework described in the previous section.

The carbon isotope composition of aquatic organic matter is primarily determined by the $\delta^{13}C$ of lake water dissolved inorganic carbon (DIC), which is influenced by isotopic exchange with atmospheric $CO_2$, input of DIC from the catchment, $^{13}C$-enrichment deriving from preferential uptake of $^{12}C$ by phytoplankton during photosynthesis, recycling of $^{13}C$-depleted carbon from the decay of organic matter in the water column and bottom sediments, and $CO_2$ evasion under the low atmospheric pressure at a 4300 m elevation. Isotopic fractionation between the carbon source and the organic substrate typically results in a kinetic isotopic shift on the order of $-20‰$ in organic matter synthesized by $C_3$ plants, although this value can vary considerably depending on the concentration of dissolved $CO_2$, $HCO_3^-$ uptake, and temperature (Hollander and McKenzie, 1991; Aravena et al., 1992).

Variables that influence the nitrogen isotope composition of aquatic organic matter include the isotopic signature of available nitrogen reservoirs used by phytoplankton, nitrogen isotope fractionation, and transformations in the water column and sediments, such as denitrification and ammonia volatilization, which lead to $^{15}N$-enrichment of the residual dissolved inorganic nitrogen (DIN) pool. Strong kinetic effects can occur during nitrate and ammonium assimilation, although isotopic fractionation may not be significant in environments where DIN is limiting or during fixation of atmospheric $N_2$ (Fogel and Cifuentes, 1993; Goericke et al., 1994; François et al., 1996).

In the lower part of the LTCK sediment record spanning Units 1 and 2, $\delta^{13}C_{org}$ and $\delta^{13}C_{cell}$ values increase by about 1% whereas $\delta^{15}N$ values decrease by about 3%. Increased primary productivity, as suggested by increased OC and biogenic $SiO_2$ concentration (Fig. 4), likely account for the carbon isotope trend owing to photosynthesis-driven $^{13}C$-enrichment of DIC and/or reduced carbon isotope fractionation caused by a declining dissolved $CO_2$ concentration. Variations in lake productivity commonly provide the dominant signal preserved in the $\delta^{13}C$ of lacustrine organic matter (e.g. McKenzie, 1985; Schelske and Hodell, 1991; Meyers et al., 1993). A similar increase in the $\delta^{15}N_{org}$ record might be expected due to selective uptake of $^{14}N$ which would have led to $^{15}N$-enrichment of residual DIN. This is not the case, probably because nitrogen is limiting during times of high productivity in the oligotrophic system leading to an increase in the abundance of N-fixing algae, whose $\delta^{15}N$ values tend to closely reflect that of atmospheric $N_2$ (i.e. 0%; Collister and Hayes, 1991).

Unit 3 is characterized by fluctuating, but overall high values for carbon, nitrogen, and biogenic silica suggesting higher lake productivity relative to Unit 2 (Fig. 4). However, $\delta^{13}C_{org}$ and $\delta^{13}C_{cell}$ values are lower probably because of the influence of $^{13}C$-depleted soil-derived DIC supplied to the lake via snowmelt, groundwater, and/or overland flow. Hydrologic dilution of photosynthetically-driven $^{13}C$-enrichment in lake sediments has recently been documented in several other studies (Aravena et al., 1992; Wolfe et al., 1996, 1999, 2000), underscoring the importance of understanding the paleohydrological record for the interpretation of lake sediment carbon isotope profiles. Similarly, the increase in $\delta^{15}N_{org}$ may also reflect increased DIN availability derived from hydrologic input and a corresponding decline in N-fixers. Preferential loss of some N may have also contributed to the increase in $\delta^{15}N$ values, as suggested by the increase in C/N values, which appears to be inconsistent with an increase in terrestrial organic matter.

Oxidation of organic matter in Unit 4, caused by low lake-levels and subaerial exposure, is evident in the low concentrations of C and N (Fig. 4). Lipid biomarker composition and abundance suggests poor preservation of organic material over this interval (Polissar, 1999). Both $\delta^{13}C_{org}$ and $\delta^{15}N_{org}$ become more positive in this unit, likely because of preferential microbial breakdown of organic constituents containing weaker $^{12}C$ and $^{14}N$ bonds. Similar degradational changes in $\delta^{13}C$ and $\delta^{15}N$ have been observed in water column profiles of suspended marine sediment (Saino and Hatori, 1980; Altabet and McCarthy, 1986), blue-green algal mats (Behrens and Frishman, 1971) and peat (Macko et al., 1991). Notably, $\delta^{13}C_{cell}$ shows less significant changes compared to $\delta^{13}C_{org}$, suggesting that the carbon isotope values in the cellulose fraction are not as strongly influenced by diagenetic alterations.

At about 2.3 ka B.P., increasing lake levels resulted in a brief return to nutrient conditions that appear similar to those identified for Unit 2, namely $^{13}C$-enrichment resulting from increased lake productivity, and $^{15}N$-depletion caused by an increase in abundance of $N_2$-fixers. The re-establishment of alpine glaciers in the catchment resulted in a meltwater-dominated system by about 1.4 ka B.P., with attendant changes towards lower $\delta^{13}C_{org}$ and $\delta^{13}C_{cell}$ values, and higher $\delta^{15}N_{org}$. These changes are possibly related to influxes of soil-derived $^{13}C$-depleted DIC, and an increase in DIN supply, respectively.

### 5.5. Regional paleorecords and insolation forcing

Overall, the regional paleoclimate signal appears to be consistent over century to millennial timescales across the altiplano. Fig. 8 summarizes the results from a series of records including LTCK, Lake Titicaca, Sajama, pluvial lakes on the altiplano, and the glacial history of the region.

Numerous studies on Lake Titicaca document water-level fluctuations during the Holocene and are generally consistent with the record from LTCK. Water levels in Lake Titicaca were between 50 and 85 m lower during the early and middle Holocene (Wirrmann and De Oliveira Almeida, 1987; Seltzer et al., 1998) when glaciers were absent in the LTCK watershed. Mourguiart et al. (1998) document a period of flooding at $\sim$ 8.8 ka B.P. and a dry event at $\sim$ 6.1 ka B.P. noted by arrows in Fig. 8. The flooding at $\sim$ 8.8 ka B.P. occurred just after, or possibly during, the onset of more $\delta^{18}O$-depleted lake water values in LTCK suggesting the onset of slightly wetter conditions after a very arid period during deglaciation. The dry event in Lake Titicaca at $\sim$ 6.1 ka B.P. occurred at the onset of the period of seasonal desiccation in LTCK between 6.1 and 2.3 ka B.P. (Fig. 8). Water levels rose to near the overflow level in Lake Titicaca around 3.5 ka B.P. (Mourguiart, 1990; Wirrmann et al., 1992; Wirrmann and Mourguiart, 1995; Abbott et al., 1997b; Mourguiart et al., 1998), however LTCK continued to desiccate on a seasonal basis until 2.3 ka B.P. This discrepancy suggests conditions became wetter in the northern reaches of the Lake Titicaca watershed prior to 3.5 ka B.P. while the southernmost section remained dry. A single $\delta^{18}O$ measurement from LTCK at 3.8 ka B.P. is depleted relative to the other data from Unit 4 suggesting a wet phase of short duration around this time. A marked lowstand in Lake Titicaca between 2.4 and 2.2 ka B.P. culminated around the onset of wetter conditions and the return of glaciers to the LTCK watershed after 2.3 ka B.P.

The dust record from the Sajama ice core contains four notable events indicated by arrows in Fig. 8 between 5.55 and 2.35 ka B.P. that occurred during the period when LTCK desiccated on a seasonal basis. The source of the dust is likely from the salt flats between 18 and 21°S, suggesting this arid period was a regional phenomenon. Interestingly, the most recent of these dust events occurred at 2.35 ka B.P., just prior to the onset of wetter conditions in the LTCK watershed, and after the onset of higher water levels in Lake Titicaca.

Late Pleistocene glaciation in the region culminated between 16.7 and 14.0 ka B.P. followed by deglaciation between 14.0 and 11.2 ka B.P. (Seltzer, 1990, 1992). There is no evidence for early or middle Holocene glaciation. Neoglaciation occurred after 2.3 ka in LTCK and Laguna Viscachani, also in the Cordillera Real (Seltzer, 1990; Abbott et al., 1997a).

The record from pluvial lakes in the region roughly tracks that of the glacial history. Dates for the Tauca high lake phase range from 16.2 to 13.4 ka B.P. (Clayton and Clapperton, 1997) or to 12.3 ka B.P. (Grosjean et al., 1995). A second high lake phase, the Coipasa event, occurred between 10.5 and 9.5 ka B.P. (Sylvestre et al., 1999). The magnitude of the second event was considerably smaller and of shorter duration. Both the record of the glacial history and the pluvial lakes indicate arid conditions in the region after the last local glacial maximum at approximately 16.2 ka B.P. (Clayton and Clapperton, 1997).

We hypothesized previously that lower summer insolation during the early and middle Holocene resulted in decreased summer precipitation and arid conditions on the altiplano (Abbott et al., 1997a; Martin et al., 1997; Seltzer et al., 2000). Likewise, increased winter insolation appears to have resulted in enhanced melting during winter months. We contend that during the Holocene, when boundary conditions were not affected by changes in global ice volume or fluctuating sea level, millennial-scale shifts in the monthly distribution of insolation drove changes in the P–E balance across the equatorial region. For example, during the middle Holocene, when summer (January) insolation at 20°S was 4–6% lower relative to present, a marked dry phase occurred that resulted in a $>$ 50 m lowering of Lake Titicaca

(Wirrmann and Fernando De Oliveira, 1987; Seltzer et al., 1998; Cross et al., 2000). At the same time, alpine glaciers disappeared from catchments lower than 5500 m (Abbott et al., 1997a). Corroborating evidence comes from the northern hemisphere tropics, where middle Holocene winter insolation (January) at 10°N was 4 to 6% greater than today, resulting in conditions wetter than any other period in the past 12 ka (Hodell et al., 1991).

During the late Holocene, water levels in Lake Titicaca record an overall rising trend with renewed cirque glacier activity in the Cordillera Real. Accumulation on Sajama increased concomitantly (Thompson et al., 1998). Wetter periods apparently result from enhanced convection driven by increased summer insolation. Greater precipitation likely resulted from increased seasonality resulting in warmer summers and cooler winters and increased sea-level pressure over the ocean and decreased sea-level pressure over land, resulting in increased water-vapor transport over the continent. Increased summer precipitation coupled with increased summer cloudiness and decreased winter insolation therefore result in an increase in the net P–E balance. This is supported by the work of Francou et al. (1995) and Ribstein et al. (1995) that shows increase in modern-day meltwater production from the Zongo Glacier during years with lower precipitation, since reduced cloud cover results in increased incident solar radiation, causing warmer temperatures and enhanced ablation. In contrast, years with higher precipitation have more cloud cover and lower incident radiation, leading to cooler temperatures and lower melting rates. Kull and Grosjean (1998) show the importance of albedo changes to climate illustrating that clearly other factors are important influences on precipitation.

## 6. Conclusions

The implication of this multiproxy investigation is that Holocene environmental conditions in the Cordillera Real were highly dynamic on centennial to millennial time-scales. Concordant isotopic and biological proxies, including down-core variability of cellulose-inferred $\delta^{18}o_{lw}$ values on the order of 10‰, indicate that fundamental changes in paleohydrological regimes occurred several times during the Holocene. Comparison of the LTCK record with other paleoclimate records in the region illustrates a consistent overall pattern of aridity from the late glacial through the middle Holocene. The effect of changing insolation patterns on precipitation appears to govern broadly the late glacial and middle Holocene aridity at the regional scale, but does not explain the century-scale variability that demonstrably exists. Furthermore, there is a notable discrepancy between the timing of water level rise in Lake Titicaca around 3.5 ka B.P and the onset of wetter conditions in the LTCK watershed at 2.3 ka B.P. This suggests wetter conditions occurred in the northern reaches of the Titicaca watershed first resulting in rising water levels in Lake Titicaca while LTCK continued to desiccate seasonally. Finally, we note that the last 2.3 ka has been the wettest period during the Holocene on the altiplano and adjacent cordillera, resulting in the re-inception and subsequent growth of alpine glaciers. This is an especially important point, given the high sensitivity of the region to climatically induced hydrological changes, a rapidly growing population, and limited water resources, especially during the winter dry season, when glacial meltwater is an important source of water for municipal use and electrical production.

## Acknowledgements

We thank Donald Rodbell and Pratigya Polissar for their assistance in the field and Bruce Finney for his analyses of vegetation and sediment samples. We thank Lonnie Thompson for supplying the data from the Sajama ice core. Emi Ito and Platt Bradbury worked very hard to help us revise an earlier manuscript, and deserve special thanks. This research was funded by NSF grant ATM-9632267 to M.B. Abbott and ATM-9613991 to G.O. Seltzer.

## Appendix A. Diatoms identified from the LTCK core.

*Achnanthes hungarica* Grun.
*Achnanthes kuelbsii* Lange-Bertalot
*Achnanthes lanceolata* (Bréb.) Grun.
*Achnanthes laterostrata* Hust.
*Achnanthes levanderi* Hust.
*Achnanthes minutissima* Kütz.
*Achnanthes minutissima* var. *macrocephala* Hust.
*Achnanthes montana* Krasske
*Achnanthes peragalli* Brun and Héribaud
*Achnanthes rossi* Hust.
*Achnanthes saccula* Carter
*Achnanthes* spp.
*Amphora libyca* Ehr.
*Amphora perpusilla* Grun.
*Aulacoseira alpigena* (Grun.) Krammer
*Brachysira vitrea* (Grun.) Ross in Hartley
*Brachysira zellensis* (Grun.) Round and Mann
*Cocconeis diminuta* Pant.
*Cocconeis placentula* var. *lineata* (Ehr.) VanH.
*Craticula halophila* (Grun. ex VanH.) Mann
*Cyclotella stelligera* (Cleve and Grun. in Cleve) VanH.
*Cymbella affinis* Kütz.
*Cymbella angustata* (W.Sm.) Cleve
*Cymbella cistula* (Ehr. in Hempr. and Ehr.) Kirchner
*Cymbella gracilis* (Rabh.) Cleve
*Cymbella minuta* Hilse ex Rabh.
*Denticula kuetzingii* Grun.

*Diploneis ovalis* (Hilse) Cleve
*Epithemia adnata* (Kütz.) Bréb.
*Eunotia hexaglyphis* Ehr.
*Eunotia incisa* Greg.
*Eunotia naegelii* Migula
*Eunotia pectinalis* var. *ventricosa* Grun.
*Eunotia pectinalis* var. *minor* (Grun.) Rabh.
*Eunotia* spp.
*Fragilaria capucina* Desmaz.
*Fragilaria construens* var. *venter* (Ehr.) Grun.
*Fragilaria leptostauron* (Ehr.) Hust.
*Fragilaria microstriata* Marciniak
*Fragilaria pinnata* Ehr.
*Fragilaria pinnata* var. *lancettula* (Schumann) Hust.
*Fragilaria virescens* Ralfs
*Gomphonema acuminatum* Ehr.
*Gomphonema dichotonum* Kütz.
*Gomphonema gracile* Ehr.
*Gomphonema parvulum* Kütz.
*Gomphonema pumilum* (Grun.) Reichardt and Lange-Bertalot
*Gomphonema* spp.
*Krasskella kriegeriana* (Krasske) Ross and Sims
*Navicula atomus* (Kütz.) Grun.
*Navicula capitata* var. *hungarica* (Grun.) Ross
*Navicula cryptotenella* Lange-Bertalot
*Navicula gastrum* (Ehr.) Kütz.
*Navicula mutica* Kütz.
*Navicula pseudoscutiformis* Hust.
*Navicula pupula* Kütz.
*Navicula radiosa* Kütz.
*Navicula rhynchocephala* Kütz.
*Navicula schoenfeldii* Hust.
*Navicula* spp.
*Nitzschia amphibia* Grun.
*Nitzschia dissipata* (Kütz.) Grun.
*Nitzschia gracilis* Hantzsch
*Nitzschia hantzschiana* Rabh.
*Nitzschia romana* Grun.
*Nizschia frustulum* (Kütz.) Grun.
*Nupela* spp.
*Pinnularia abaujensis* (Pant.) Ross
*Pinnularia borealis* Ehr.
*Rhopalodia gibba* (Ehr.) O. Müller
*Stauroneis anceps* Ehr.
*Surirella ovalis* Bréb.
*Surirella ovata* Kütz.
*Synedra parasitica* (W.Sm.) Hust.
*Synedra ulna* Ehr.
*Synedra* spp.

## References


Abbott, M.B., Seltzer, G.O., Kelts, K.R., Southon, J., 1997a. Holocene Paleohydrology of the Tropical Andes from Lake Records. Quaternary Research 47, 70–80.

Abbott, M.B., Binford, M.W., Brenner, M., Kelts, K.R., 1997b. A 3500 $^{14}$C yr high-resolution record of lake level changes in Lake Titicaca, Bolivia/Peru. Quaternary Research 47, 169–180.

Aceituno, P., Montecinos, A. 1993. Circulation anomalies associated with dry and wet periods in the South American Altiplano, Fourth International Conference on Southern Hemisphere Meteorology and Oceanography, American Meteorological Society, pp. 330–331.

Altabet, M.A., McCarthy, J.J., 1986. Vertical patterns in $^{15}$N natural abundance in PON from the surface waters of warm-core rings. Journal of Marine Research 44, 185–201.

Aravena, R., Warner, B.G., MacDonald, G.M., Hanf, K.I., 1992. Carbon isotopic compositions of lake sediments in relations to lake productivity and radiocarbon dating. Quaternary Research 37, 333–345.

Aravena, R., Suzuki, O., Pena, H., Pollastri, A., Fuenzalida, H., Grilli, A., 1999. Isotopic composition and origin of the precipitation in Northern Chile. Applied Geochemistry 14, 89–100.

Aucour, A.M., Hillaire-Marcel, C., Bonnefille, R., 1993. A 30,000 year record of $^{13}$C and $^{18}$O changes in organic matter from an equatorial peatbog. In: Swart, P.K., Lohmann, K.C., McKenzie, J., Savin, S. (Eds.), Climate change in continental Isotopic Records, Vol. 78. American Geophysical Union Geophysical Monograph, pp. 343–351.

Behrens, E.W., Frishman, S.A., 1971. Stable carbon isotopes in blue-green algal mats. Journal of Geology 79, 95–100.

Berger, A., 1978a. Long-term variations of daily insolation and Quaternary climatic changes. Journal of Atmospheric Science 35, 2362–2367.

Berger, A. 1978b. A simple algorithm to compute long term variations of daily or monthly insolation. Contribution No. 18, Université Catholique de Louvian, Institut d'Astronomie et de Geophysique, G. Lemaitre, Louvian-la-Neuve, B-1348 Belgique.

Berger, A., Loutre, M.F., 1991. Insolation values for the climate of the last 10 million years. Quaternary Science Reviews 10, 297–317.

Beuning, K.R.M., Kelts, K., Ito, E., Johnson, T.C., 1997. Paleohydrology of Lake Victoria, East Africa, inferred from $^{18}$O/$^{16}$O ratios in sediment cellulose. Geology 25, 1083–1086.

Binford, M.W., Kolata, A.L., Brenner, M., Janusek, J., Abbott, M.B., Curtis, J., 1997. Climate variation and the rise and fall of an Andean civilization. Quaternary Research 47, 171–186.

Clayton, J.D., Clapperton, C.M., 1997. Broad synchrony of a late-glacial glacier advance and the highstand of paleolake Tauca in the Bolivian Altiplano. Journal of Quaternary Science 12, 169–182.

Coleman, M.L., Shepherd, T.J., Durham, J.J., Rouse, J.E., Moore, G.R., 1982. Reduction of water with zinc for hydrogen isotope analysis. Analytical Chemistry 54, 993–995.

Collister, J.W., Hayes, J.M., 1991. A preliminary study of the carbon and nitrogen isotope biogeochemistry of lacustrine sedimentary rocks from the Green River Formation, Wyoming, Utah and Colorado. United States Geological Survey Bulletin, 1973-A-G, C1–C16.

Coudrain-Ribstein, A., Prats, B., Quintanilla, J., Zuppi, G.M., Cahuaya, D., 1995. Salinidad del recurso hidrico subterraneo del Altiplano Central. Bull. Inst. Fr. Studes Andines 24, 483–493.

Cross, S.L., Baker, P.A., Seltzer, G.O., Fritz, S.C., Dunbar, R.B., 2000. A new estimate of the Holocene lowstand level of Lake Titicaca, implications for tropical paleohydrology. The Holocene 10, 21–32.

DeMaster, D.J., 1981. The supply and accumulation of silica in the marine environment. Geochemica et Cosmochimica Acta 45, 1715–1732.

DeNiro, M.J., Epstein, S., 1981. Isotopic composition of cellulose from aquatic organisms. Geochemica et Cosmochimica Acta 42, 495–506.

Duthie, H.C., Yang, J.R., Edwards, T.W.D., Wolfe, B.B., Warner, B.G., 1996. Hamilton Harbor, Ontario: 8300 years of limnological and environmental change inferred from microfossil and isotopic analysis. Journal of Paleolimnology 15, 79–97.

Edwards, T.W.D., Buhay, W.M., Elgood, R.J., Jiang, H.B., 1994. An improved nickel-tube pyrolysis method for oxygen isotope analysis of organic matter and water. Chemical Geology (Isotope Geoscience Section) 114, 179–183.

Edwards, T.W.D., Elgood, R.J., Wolfe, B.B., 1997. Cellulose extraction from lake sediments for $^{18}O/^{16}O$ and $^{13}C/^{12}C$ analysis. In: Environmental Isotope Laboratory Technical Procedure 28.0. University of Waterloo, Waterloo, 4 pp.

Edwards, T.W.D., McAndrews, J.H., 1989. Paleohydrology of a Canadian Shield lake inferred from $^{18}O$ in sediment cellulose. Canadian Journal of Earth Sciences 26, 1850–1859.

Edwards, T.W.D., Wolfe, B.B., MacDonald, G.M., 1996. Influence of changing atmospheric circulation on precipitation $^{18}O$-temperature relations in Canada during the Holocene. Quaternary Research 46, 211–218.

Epstein, S., Mayeda, T.K., 1953. Variations in the $^{18}O/^{16}O$ ratio in natural waters. Geochimica et Cosmochimica Acta 4, 213.

Epstein, S., Thompson, P., Yapp, C.J., 1977. Oxygen and hydrogen isotopic ratios in plant cellulose. Science 198, 1209–1215.

Fisher, M.M., Brenner, M., Reddy, K.R., 1992. A simple, inexpensive piston corer for collecting undisturbed sediment/water interface profiles. Journal of Paleolimnology 7, 157–161.

Fogel, M.L., Cifuentes, L.A., 1993. Isotope fractionation during primary production. In: Engel, M.H., Macko, S.A. (Eds.), Organic Geochemistry. Plenum Press, New York, pp. 73–98.

François, R., Pilskaln, C.H., Altabet, M.A., 1996. Seasonal variation in the nitrogen isotopic composition of sediment trap materials collected in Lake Malawi. In: Johnson, T.C., Odada, E.O. (Eds.), The Limnology, Climatology and Palaeoclimatology of the East African Lakes. Gordon and Breach, Amsterdam, pp. 241–250.

Francou, B., Ribstein, P., Saravia, R., Tiriau, E., 1995. Monthly balance and water discharge of an inter-tropical glacier: Zongo Glacier, Cordillera Real, Bolivia 16°S. Journal of Glaciology 41, 61–67.

Fritz, P., Suzuki, O., Silva, C., Salati, E., 1981. Isotope Hydrology of groundwaters in the Pampa del Tamarugal, Chile. Journal of Hydrology 53, 161–184.

Germain, H., 1981. Flore des diatomées, eaux douces et saumâtres du Massif Armoricain et des contrées voisines d'Europe occidentale. Société Nouvelle des Éditions Boubée, Paris, 444 pp.

Goericke, R., Montoya, J.P., Fry, B., 1994. Physiology and isotopic fractionation in algae and cyanobacteria. In: Lajtha, K., Michener, R.H. (Eds.), Stable Isotopes in Ecology and Environmental Science. Blackwell, Oxford, pp. 187–221.

Gonfiantini, R., 1986. Environmental isotopes in lake studies. In: Fritz, P., Fontes, J.C. (Eds.), Handbook of Environmental Isotope Geochemistry, Vol. 2. Elsevier, New York, USA, pp. 113–168.

Gouze, P., Argollo, J., Saliege, J.-F., Servant, M., 1986. Interprétation paléoclimatique des oscillations des glaciers au cours des 20 derniers millénaires dans les régions tropicales: exemple des Andes Boliviennes. Comptes Rendus de L'Académie des Sciences Paris, Série II 303, 219–223.

Grootes, P.M., Stuiver, M., Thompson, L.G., Mosley-Thompson, E., 1989. Oxygen isotope changes in tropical ice. Quelccaya, Peru. Journal of Geophysical Research 94, 1187–1194.

Grosjean, M., 1994. Paleohydrology of the Laguna Lejía (north Chilean Altiplano) and climatic implications for late-glacial times. Palaeogeography, Palaeoclimatology, Palaeoecology 109, 89–100.

Grosjean, M., Geyh, M.A., Messerli, B., Schotterer, U., 1995. Late-glacial and early Holocene lake sediments, ground-water formation and climate in the Atacama Altiplano 22–24°S. Journal of Paleolimnology 14, 241–252.

Hill, M.O., Gauch, H.G., 1980. Detrended Correspondence Analysis: an improved ordination technique. Vegetatio 42, 47–58.

Hodell, D.A., Curtis, J.H., Jones, G.A., Higuera-Gundy, A., Brenner, M., Binford, M.W., Dorsey, K.T., 1991. Reconstruction of Caribbean climate change over the past 10,500 years. Nature 352, 790–793.

Hodell, D.A., Curtis, J.H., Brenner, M., 1995. Possible role of climate in the collapse of Classic Maya civilization. Nature 375, 391–394.

Hodell, D.A., Schelske, C.L., 1998. Production, sedimentation, isotopic composition of organic matter in Lake Ontario. Limnology and Oceanography 43, 200–214.

Hoffman, J.A.J. 1975. Climatic Atlas of South America. World Meteorological Organization, Ginebra, Hungary.

Hollander, D.J., McKenzie, J.A., 1991. $CO_2$ control on carbon-isotope fractionation during aqueous photosynthesis: a paleo-$pCO_2$ barometer. Geology 19, 929–932.

Hostetler, S.W., Giorgi, F., 1992. Use of a regional atmospheric model to simulate lake-atmosphere feedbacks associated with Pleistocene Lakes Lahontan and Bonneville. Climate Dynamics 7, 39–44.

Hustedt, F., 1959. Die Kieselalgen Deutschlands, Österreichs und der Schweiz, Teil II.. In: Rabenhorst, T. (Ed.), Kryptogamen-Flora von Deutschland. Österreich und der Schweizg. Academische Verlagsgesellschaft, Leipzig, 845 pp.

Kessler, A., 1988. Die Schwankungen des Wasserhaushaltes de südamerikanischen Altiplano und das Weltklima v. Jahrbuch der Geographischen Gesellschaft zu Hannover 139–159.

Kovach, (1993). MVSP Plus Version 2.1 users' manual addendum. Kovach Computing Services, Aberystwyth, U.K, pp 16.

Krammer, K., Lange-Bertalot, H., 1986–1991. Bacillariophyceae 1 Teil: Naviculaceae, 876 pp. (1986); 2 Teil: Bacillariaceae, Epithemiaceae, Surirellaceae, 596 pp. (1988); 3 Teil: Centrales, Fragilariaceae, Eunotiaceae, 576 pp. (1991a); 4 Teil: Achnanthaceae, Kritische Ergänzungen zu Navicula (Lineolatae) und Gomphonema Gesamtliteraturverzeichnis, 437 pp. (1991b) In: Ettl, H., Gerloff, H., Heynig H., Mollenhauer D. (Eds.), Sübwasserflora von Mitteleuropa 2/1–4. Gustav Fischer, Stuttgart.

Kull, C., Grosjean, M., 1998. Albedo change, Milankovitch forcing, late Quaternary climate changes in the central Andes. Climate Dynamics 14, 871–881.

MacDonald, G.M., Edwards, T.W.D., Moser, K.A., Pienitz, R., Smol, J.P., 1993. Rapid response of treeline vegetation and lakes to past climate warming. Nature 361, 243–246.

Macko, S.A., Engel, M.H., Hartley, G., Hatcher, P., Helleur, R., Jackman, P., Silfer, J.A., 1991. Isotopic compositions of individual carbohydrates as indicators of early diagenesis of organic matter in peats. Chemical Geology 93, 147–161.

Martin, L., Bertaux, J., Correge, T., Ledru, M.P., Mourguiart, P., Sifeddine, A., Soubies, F., Wirrmann, D., Sugiro, K., Turcq, B., 1997. Astronomical forcing of contrasting changes in Tropical South America between 12,400 and 8800 cal yr B.P. Quaternary Research 47, 117–122.

McKenzie, J.A., 1985. Carbon isotopes and productivity in the lacustrine and marine environment. In: Stumm, W. (Ed.), Chemical Processes in Lakes. Toronto, Wiley, pp. 99–118.

Mercer, J.H., Palacios, O., 1978. Radiocarbon dating of the last glaciation in Peru. Geology 5, 600–604.

Meyers, P.A., Takemura, K., Horie, S., 1993. Reinterpretation of Late Quaternary sediment chronology of Lake Biwa, Japan, from correlation with marine glacial-interglacial cycles. Quaternary Research 39, 154–162.

Mourguiart, P., 1990. Une approche nouvelle du problème posé par les reconstrutions des paléoniveaux lacustres: utilisation d'une fonction de transfert basée sur les faunes d'ostracodes. Géodynamique 5, 151–166.

Mourguiart, P., Correge, T., Wirrmann, D., Argollo, J., Montenegro, M.E., Pourchet, M., Carbonel, P., 1998. Holocene paleohydrology of Lake Titicaca estimated from an ostracod-based transfer function. Palaeogeography Palaeoclimatology Palaeoecology 143, 51–72.

Patrick, R., Reimer, C.W., 1966. The Diatoms of the United States exclusive of Alaska and Hawaii. Academy of Natural Sciences of Philadelphia Monograph 13, Vol. 1. 688 pp.

Patrick, R., Reimer, C.W., 1975. The Diatoms of the United States exclusive of Alaska and Hawaii. Academy of Natural Sciences of Philadelphia Monograph 13, Vol. 2 Part 1. 213 pp.

Polissar, P.J., 1999. Lipid biomarker, elemental and isotopic evidence for lacustrine organic matter preservation and source: Lago Taypi Chaka Kkota, Bolivia. Masters Thesis, University of Massachusetts.

Ribstein, P., Tiriau, E., Francou, B., Saravia, R., 1995. Tropical climate and glacier hydrology: a case study in Bolivia. Journal of Hydrology 165, 221–234.

Roche, M.A., Bourges, J.C., Mattos, R., 1992. Climatology and hydrology of the Lake Titicaca basin. In: Dejoux, C., Iltis, A. (Eds.), Lake Titicaca: a Synthesis of Limnological Knowledge. Kluwer Academic Publishers, Boston, pp. 63–83.

Saino, T., Hatori, A., 1980. $^{15}N$ natural abundance in oceanic suspended particle matter. Nature 283, 752–754.

Schelske, C.L., Hodell, D.A., 1991. Recent changes in productivity and climate of Lake Ontario detected by isotopic analysis of sediments. Limnology and Oceanography 36, 961–975.

Seltzer, G.O., 1990. Recent glacial history and paleoclimate of the Peruvian-Bolivian Andes. Quaternary Science Reviews 9, 137–152.

Seltzer, G.O., 1992. Late Quaternary glaciation of the Cordillera Real, Bolivia. Quaternary Science Reviews 7, 87–98.

Seltzer, G.O., Cross, S., Baker, P., Dunbar, R., Fritz, S., 1998. High-resolution seismic reflection profiles from Lake Titicaca, Peru/Bolivia: evidence for Holocene aridity in the tropical Andes. Geology 26, 167–170.

Seltzer, G.O., Rodbell, D.T., Burns, S., 2000. Isotopic evidence for late Quaternary climatic change in tropical South America. Geology 28, 35–38.

Servant, M., Fontes, J.-C., 1978. Les lacs quaternaires des hauts plateaux des Andes Boliviennes: premieres interpretations paleoclimatiques. Cahiers ORSTOM, Serie Geologie 10, 9–23.

Sternberg, L.S.L., 1989. Oxygen and hydrogen isotope ratios in plant cellulose; mechanisms and applications. In: Rundel, P.W., Ehleringer, J.R., Nagy, K.A. (Eds.), Stable Isotopes in Ecological Research. Springer, New York, pp. 124–141.

Stimson, J., 1991. Isotopic and geochemical evolution of groundwaters in Cochabamba Valley, Bolivia. Masters Thesis, University of Waterloo.

Stimson, J., Frape, S.K., Drimmie, R.J., Rudolph, D.L., 1993. Causes of groundwater salinization in a low-lying area of Cochabamba, Bolivia. In: Isotope Techniques in Studying Past and Current Environmental Changes in the Hydrosphere and the Atmosphere. Proceeding of an International Symposium, IAEA-SM-329, pp. 185–198.

Stuiver, M., Reimer, P.J., Bard, E., Beck, J.W., Burr, G.S., Hughen, K.A., Kromer, B., McCormac, F.G., v. d. Plicht, J., Spurk, M., 1998. INTCAL98 Radiocarbon age calibration 24,000-0 cal BP. Radiocarbon 40, 1041–1083.

Sylvestre, F., Servant, M., Servant-Vildary, S., Causse, C., Fournier, M., Ybert, J.P., 1999. Lake-level chronology on the southern Bolivian Altiplano (18°–23°S) during late-glacial time and the early Holocene. Quaternary Research 51, 54–66.

Talbot, M.R., Johannessen, T., 1992. A high resolution paleoclimatic record for the last 27,500 years in tropical West Africa from the carbon and nitrogen isotopic composition of lacustrine organic matter. Earth and Planetary Science Letters 110, 23–37.

ter Braak, C.J.F., 1987. Ordination. In: Jongman, R.H.G., ter Braak, C.J.F., VanTongeren, O.F.R (Eds.), Data Analysisi in Community and Landscape Ecology. Pudoc, Wageningen, pp. 91–173.

Thompson, L.G., Mosley-Thompson, E., Morales, B., 1984. El Niño Southern Oscillation events recorded in the stratigraphy of the tropical Quelccaya ice cap, Peru. Science 226, 50–53.

Thompson, L.G., Davis, M.E., Mosley-Thompson, E., Sowers, T.A., Henderson, K.A., Zagorodnov, V.S., Lin, P.-N., Mikhalenko, V.N., Campen, R.K., Bolzan, J.F., Cole-Dai, J., Francou, B., 1998. A 25,000-year tropical climate history from Bolivian ice cores. Science 282, 1858–1864.

Wirrmann, D., Fernando De Oliveira Almeida, L., 1987. Low Holocene level (7700 to 3650 years ago) of Lake Titicaca (Bolivia). Palaeogeography, Palaeoclimatology, Palaeoecology 59, 315–323.

Wirrmann, D., Mourguiart, P., 1995. Late Quaternary spatio-temporal limnological variations in the Altiplano of Bolivia and Peru. Quaternary Research 43, 344–354.

Wirrmann, J.P., Ybert, J.P., Mourguiart, P., 1992. A 20,000 years paleohydrological record from Lake Titicaca. In: Dejoux, C., Iltis, A. (Eds.), Lake Titicacaa Synthesis of Limnological Knowledge. Kluwer Academic Publishers, Boston, pp. 40–48.

Wolfe, A.P., 1997. On diatom concentrations in lake sediments: results of an inter-laboratory comparison and other experiments performed on a uniform sample. Journal of Paleolimnology 18, 61–66.

Wolfe, B.B., Edwards, T.W.D., 1997. Hydrologic control on the oxygen-isotope relation between sediment cellulose and lake water, western Taimyr Peninsula, Russia: implications for the use of surface-sediment calibrations in paleolimnology. Journal of Paleolimnology 18, 283–291.

Wolfe, B.B., Edwards, T.W.D., Aravena, R., 1999. Changes in carbon and nitrogen cycling regimes during tree-line retreat recorded in the isotopic content of lacustrine organic matter, western Taimyr Peninsula Russia. The Holocene 9, 215–222.

Wolfe, B.B., Edwards, T.W.D., Aravena, R., MacDonald, G.M., 1996. Rapid Holocene hydrologic change along boreal treeline revealed by $\delta^{13}C$ and $\delta^{18}O$ in organic lake sediments. Northwest Territories, Canada. Journal of Paleolimnology 15, 171–181.

Wolfe, B.B., Edwards, T.W.D., Duthie, H.C., 2000. A 6000-year record of interaction between Hamilton Harbour and Lake Ontario: quantitative assessment of recent hydrologic disturbance using $^{13}C$ in lake sediment cellulose. Aquatic Ecosystem Health and Management 3, 47–54.

Wright, H.E., Mann, D.H., Glaser, P.H., 1984. Piston corers for peat and lake sediments. Ecology 65, 657–659.

Yakir, D., 1992. Variations in the natural abundance of oxygen 18 and deuterium in plant carbohydrates. Plant Cell Environment 15, 1005–1020.